Dictyostelium Myosin I Double Mutants Exhibit Conditional Defects in Pinocytosis

Kristine D. Novak, Michelle D. Peterson, Mary C. Reedy, and Margaret A. Titus

Department of Cell Biology, Duke University Medical Center, Durham, North Carolina 27710

Abstract. The functional relationship between three *Dictyostelium* myosin Is, myoA, myoB, and myoC, has been examined through the creation of double mutants. Two double mutants, *myoA*$^-$/*B*$^-$ and *myoB*$^-$/*C*$^-$, exhibit similar conditional defects in fluid-phase pinocytosis. Double mutants grown in suspension culture are significantly impaired in their ability to take in nutrients from the medium, whereas they are almost indistinguishable from wild-type and single mutant strains when grown on a surface. The double mutants are also found to internalize gp126, a 116-kD membrane protein, at a slower rate than either the wild-type or single mutant cells. Ultrastructural analysis reveals that both double mutants possess numerous small vesicles, in contrast to the wild-type or myosin I single mutants that exhibit several large, clear vacuoles. The alterations in fluid and membrane internalization in the suspension-grown double mutants, coupled with the altered vesicular profile, suggest that these cells may be compromised during the early stages of pinocytosis, a process that has been proposed to occur via actin-based cytoskeletal rearrangements. Scanning electron microscopy and rhodamine–phalloidin staining indicates that the myosin I double mutants appear to extend a larger number of actin-filled structures, such as filopodia and crowns, than wild-type cells. Rhodamine-phalloidin staining of the F-actin cytoskeleton of these suspension-grown cells also reveals that the double mutant cells are delayed in the rearrangement of cortical actin-rich structures upon adhesion to a substrate. We propose that myoA, myoB, and myoC play roles in controlling F-actin filled membrane projections that are required for pinosome internalization in suspension.

CELL movements produced in the cell cortex beneath the plasma membrane are essential for phagocytosis, directed cell movement, nutrient and hormone uptake, and cell shape changes. The cell cortex is rich in actin, and it has been proposed that actin polymerization and/or actin-based motors (i.e., myosins) generate the force required to accomplish these various tasks. The identification of the motors involved is critical for understanding the molecular basis of these cellular movements.

Cells express multiple classes of myosins (Bement et al., 1994*a*), and each type is proposed to carry out a specific role within the cell. Myosin Is have been identified in many cell types, from amoebae to vertebrates, including human cell lines and yeast (Pollard and Korn, 1973; Goodson and Spudich, 1995; Bement et al., 1994*b*). They have been proposed to play a role in the formation of pseudopodia and lamellipodia and in the maintenance of the apical cytoskeleton in intestinal epithelial cells (Fukui et al., 1989; Mooseker et al., 1991; Wagner et al., 1992).

Immunofluorescence localizations performed with myosin I-specific antibodies implicate this motor in mediating events at the plasma membrane/cytoskeleton interface. Bovine adrenal myosin I antibody stained the cell periphery, filopodia, lamellipodia and growth cones in kidney, brain, PC12, Swiss 3T3, and CHO cells (Wagner et al., 1992). Myosin I is associated with vesicles in enterocytes (Drenckhahn and Dermietzel, 1988). Golgi-derived vesicles from epithelial cells have myosin I on their surface where it is proposed to move these vesicles through the actin-rich cytoskeleton to the apical plasma membrane (Fath and Burgess, 1993). *Acanthamoeba* myosin Is localized to the cell cortex, plasma membrane, and large vacuole membranes (Baines and Korn, 1990; Baines et al., 1992; Yonemura and Pollard, 1992). Similarly, myosin Is from *Dictyostelium* have been localized to cell membranes, phagocytic cups, and at leading edges of locomoting cells (Fukui et al., 1989; Jung et al., 1993), suggesting that myosin I in eukaryotes plays a role in the dynamics of actin-rich, membrane-associated cortical structures.

The role of amoeboid myosin Is in vivo has been addressed using the simple eukaryote *Dictyostelium* as a model system. *Dictyostelium* undergo cell movements that can be easily quantified, such as pinocytosis, phagocytosis, and cell division. Six *Dictyostelium* genes encoding myosin Is, *myoA-F*, have been identified (Jung et al., 1989, 1993; Titus et al., 1989, 1995; Urrutia et al., 1993; Peterson et al.,

Address all correspondence to Margaret Titus, Dept. of Cell Biology, Duke University Medical Center, Durham, NC 27710. Tel.: (919) 681-8859. Fax: (919) 684-5481.

1995). These motor proteins each possess a typical conserved myosin head domain, followed by a COOH-terminal polybasic domain that has been implicated in membrane binding in vitro (Adams and Pollard, 1989; Miyata et al., 1989). The *Dictyostelium* myosin Is can be divided into two types on the basis of differences in the COOH-terminal tail region. The *myoB*, *C*, and *D* genes encode "classic" myosin Is that are structurally homologous to the *Acanthamoeba* myosin Is (Jung et al., 1989; Jung et al., 1993; Peterson et al., 1995). The polybasic domain in the tail of the classic myosin I is followed by both a region rich in glycine, proline, and alanine (GPA)[1], and a *src* homology 3 domain (SH3). The GPA domain comprises a second ATP-insensitive actin-binding site that can cross-link actin filaments in vitro (Lynch et al., 1986; Doberstein and Pollard, 1992; Jung and Hammer, 1994; Rosenfeld and Rener, 1994). The SH3 domains have been found in proteins that associate with or regulate the cytoskeleton (Pawson and Gish, 1992). The *Dictyostelium* classic myosin Is have been localized to the leading edge of motile amoeboid cells (Fukui et al., 1989; Jung et al., 1993; Jung and Hammer, 1994). The other type of *Dictyostelium* myosin Is, myoA and E, are referred to as "short" myosin Is. They lack both the COOH-terminal GPA and SH3 domains, and are thus smaller than those of the classic myosin Is (Titus et al., 1989; Urrutia et al., 1993). The presence of a membrane binding site in the tail region of all myosin Is along with an SH3 domain present in the classic myosin Is further supports the theory that these motor proteins are responsible for producing forces required to move actin filaments relative to membranes.

The existence of multiple myosin I isoforms in different cell types, the identification of at least four different subclasses (Bähler et al., 1994; Morgan et al., 1994), and differences in the COOH-terminal tail regions of the myosin Is suggests that each type of myosin I mediates a specific actin-based motile function. However, *Dictyostelium* cells lacking either a classic myosin I, myoB, or a short myosin I, myoA, had surprisingly similar defects (Wessels et al., 1991; Titus et al., 1993). They both had decreased instantaneous velocities, an increased number of pseudopods, and an increased rate of turning. The defects were consistent with hypothesis that these motors play a role in mediating movements of the plasma membrane along actin filaments. Mutants lacking either myoC or myoD appeared to be normal in all cellular functions examined (Jung et al., 1993; Peterson et al., 1995). The phenotypes of the myosin I single mutants suggested that the role of a given myosin I could not be predicted on the basis of the tail sequence, and that myosin I isoforms function cooperatively. Therefore mutants that lack two myosin Is were created to determine the functional relationship between myoA, B, and C.

Materials and Methods

Standard Methods

All routine manipulations of DNA and RNA were carried out using standard methods (Ausubel et al., 1993). Total cellular RNA was prepared using RNAzol (Tel-Test, Inc., Friendswood, TX) and poly-$(A)^+$ selected using Poly-ATract mRNA Isolation System (Promega Corp., Madison, WI).

Maintenance of Stock Cultures

The parental *Dictyostelium discoideum* KAx3 axenic strain and HTD2-1, HTD2-2, HTD4-1, and HTD4-2 strains were all maintained in HL5, a nutrient medium for axenic stains (Sussman, 1987). The HTD2 and HTD4 strains are $myoA^-$ and $myoC^-$ strains, respectively, that have been previously described (Peterson et al., 1995). The thymidine auxotroph JH10 was maintained in HL5 supplemented with 100 μg/ml thymidine (Hadwiger and Firtel, 1992). All substrate-grown *Dictyostelium* strains were carried on bacteriological plastic plates in HL5. Suspension-grown cells were inoculated into 100 ml HL5 in 250-ml Erlenmeyer flasks and carried in shaking culture at 240 rpm for 72 h before an experiment.

Construction of Vectors

The full-length *myoB* gene, isolated in a screen of an Eco RI λZAP II (Stratagene, La Jolla, CA) genomic library, was excised from a phage clone as a 5.5-kb EcoRI fragment in pBluescript SK^-, resulting in a plasmid referred to as pDTb2. The neomycin gene replacement vector for the *myo*B gene was generated by first digesting pDTb2 with BclI, then gel-purifying the vector backbone, which contained mostly 5′ noncoding and 3′ noncoding sequences. A 2.1-kb BamHI/BglII fragment from pNEO-MLS^- (Manstein et al., 1989) containing the neomycin drug resistance cassette (Neo) was then ligated to the pDTb2 vector backbone, with the direction of neomycin resistance transcription opposed that of the *myo*B gene. The resulting plasmid was referred to as pDTb9R. A second gene-targeting vector, pDTb7R, was generated by ligating a 3.2-kb BamHI fragment from the pGEM26 plasmid, that carries the thymidylate synthase gene (Hadwiger and Firtel, 1992), to the same Bcl I-cut pDTb2 vector backbone as the Neo cassette.

Transformation of Dictyostelium

The transformation of *Dictyostelium* was performed following a slightly modified version (Kuspa and Loomis, 1992) of the original protocol (Howard et al., 1988). A control $myoB^-$ strain was initially generated by introducing pDTb7R into JH10 and selecting colonies that were able to grow in the absence of added thymidine. The two different myosin I double mutant strains were generated by introducing the pDTb9R plasmid into either the $myoA^-$ or $myoC^-$ single mutants (Peterson et al., 1995) and colonies selected for G418 resistance (Manstein et al., 1989). Colonies were visible within 9 d, and several independent clones were then transferred to individual 100-mm plates. A single clone was picked from each of these 100-mm plates and transferred to a second individual 100-mm plate. Transformants carrying a disrupted *myoB* gene were initially identified by western blotting, using polyclonal antibodies generated against the tail region of the myoB protein (M. A. Titus, unpublished data), and the gene disruption event was confirmed by Southern blotting. Each of the targeted myosin I genes were disrupted by recombination in the head regions between the ATP and actin binding regions. Therefore, only a very small, nonfunctional portion of the myosin head would be expressed in the unlikely situation that a truncated transcript were produced and translated. The homologous recombinants were named according to the system devised by Demerec et al. (1966): the $myoA^-/B^-$ are HDT5-1 and HTD5-2, while $myoB^-/C^-$ are HDT6-1 and HTD6-2. These strains are referred to by their colloquial names ($myoA^-/B^-$, etc.) throughout this paper. Several colonies that were G418-resistant but did not prove to have a disrupted *myoB* locus, as determined by Southern analysis, were considered nonhomologous recombinants and used as controls for the effect of the presence of the selection drug G418 in the medium.

Pinocytosis

Pinocytosis of cells in suspension culture was carried out using FITC-dextran as previously described (Klein and Satre, 1986). Fluorescence was measured on a Perkin-Elmer 650-40 fluorescence spectrophotometer (Perkin-Elmer Corp., Norwalk, CT) with an excitation wavelength of 470 nm and emission wavelength of 520 nm. A standard curve was used to calculate μl FITC-dextran per 10^6 cells.

Pinocytosis of cells on plates was carried out using the same method

1. *Abbreviations used in this paper*: CHC^-, clathrin heavy chain null cells; GPA, glycine, proline, and alanine; Neo, neomycin drug resistance cassette; SH3, src homology 3 domain.

(Klein and Satre, 1986) with a few modifications. Cells were grown to confluency on 60-mm plates, and then incubated with 2 mg/ml FITC-dextran in a total volume of 2 ml HL5. The media was exchanged for ice-cold MES buffer (20 mM 2-[*N*-morpholino] ethane sulfonic acid, pH 6.8, 2 mM $MgSO_4$, 0.2 mM $CaCl_2$) at the indicated times, and the dishes immediately placed on ice. After two washes in ice-cold MES buffer, the cells were transferred to a tube containing 10 ml of MES buffer and collected by centrifugation. The cell pellet was then resuspended in 3 ml of 50 mM Na_2HPO_4, pH 9.2, and processed as for cells from suspension.

For visualization of FITC-dextran containing vesicles, cells were incubated with FITC-dextran for 60 min. After this time, 1 ml of each cell type was collected, pelleted, and washed once gently with Sorenson's buffer (14.6 mM KH_2PO_4, 2 mM Na_2HPO_4, pH 6.5). Cells were then resuspended in 1 ml Sorenson's buffer and a small drop was placed on a coverslip. To view all vesicles in one plane of focus and improve resolution, living cells were flattened with an overlay of a thin agarose sheet as previously described (Fukui et al., 1987). Cells were then immediately photographed under fluorescent illumination using a Zeiss Axiophot (Carl Zeiss, Inc., Thornwood, NY) with a 40× plan-neofluor objective, 1.3 NA and a 2× optivar. The total number of fluorescent vesicles per cell was counted, regardless of size, for 40 KAx3 cells, 61 *myoA*$^-$/*myoB*$^-$ cells, and 100 *myoB*$^-$/*myoC*$^-$ cells. The fluorescence images were collected with a Photometrics Star 1 camera system (Photometrics Ltd., Tucson, AZ).

Phagocytosis

The measurement of bacterial uptake was performed using a modified version (Peterson et al., 1995) of a protocol previously described (Witke et al., 1992). Briefly, *Escherichia coli* B/r washed and diluted in Sorenson's phosphate buffer were incubated with cells from each of the mutant cell lines in suspension at 150 rpm. Bacterial clearing was measured by monitoring the change in optical density at 600 nm over the course of 5 h. The bacterial suspension alone was also monitored as a control and found not to decrease significantly over the course of the experiment.

Biotinylation Assay

Biotinylation of cell surface proteins was carried out using a procedure originally developed by Luna and colleagues (Ingalls et al., 1986) and modified by others to monitor the internalization of membrane proteins (Bacon et al., 1994). Cells were assayed in suspension by initially collecting 4×10^6 suspension-grown log-phase cells/sample in a prechilled rotor. The cells were washed once with 10 ml ice-cold Sorenson's buffer, pH 6.1. The cell pellets were then resuspended in 0.5 ml Sorenson's buffer, pH 8.0, containing NHS-SS-Biotin (Pierce, Rockford IL) at a final concentration of 1 mg/ml. A control unbiotinylated sample was removed before this treatment. Cells were incubated 30 min in an ice/water bath, and the biotinylation reaction was stopped by centrifugation and a 20 min incubation on ice in 0.5 ml quenching buffer. The quenching buffer contained 50 mM NH_4Cl, 1 mM $MgCl_2$, 0.1 mM $CaCl_2$, 2 mM K/$NaPO_4$ buffer, pH 6.1. The labeled cells were then washed once with 1 ml of 10% BSA in HL5 and resuspended in 0.5 ml of the same. Cells were placed in a 24°C water bath to begin the internalization process, and uptake was stopped at the indicated times by placing the cells on ice and immediately adding 0.5 ml ice-cold Sorenson's buffer containing 5% BSA. Cells were spun and washed once again with the same buffer. Samples to be stripped were spun, resuspended in 50 mM glutathione (Sigma Chemicals Co., St. Louis, MO), 75 mM NaCl, 1 mM EDTA, 75 mM NaOH, and incubated in an ice/water bath for 20 min followed by a spin, resuspension, and 30 min incubation. All samples were then washed two times in 1 ml ice-cold Sorenson's buffer.

The same internalization assay was carried out using cells grown on a surface. A total of 4×10^6 substrate-grown cells were allowed to adhere for 45 min to 60 mm plates, placed on ice, and all further incubations and washes described were performed on the plates as described as for cells in tubes. A final cell pellet was collected for cells from both suspension and substrate conditions, resuspended in nonreducing sample buffer, boiled for 3 min, run on 7.5% SDS-PAGE gels, and transferred to nitrocellulose. Nitrocellulose was blocked for at least 30 min in 6% casein, 1% PVP-40, 10 mM EDTA in PBS, and subsequently incubated for 2 h with 1 μg/ml HRP-streptavidin in the same solution. The blot was washed four times for 15 min each in 20 mM Tris, pH 7.5, 150 mM NaCl, 0.1% Tween-20. Chemiluminescence detection was carried out using HRP-labeled streptavidin and following the manufacturer's instructions for ECL (Amersham Corp., Arlington Heights, IL).

Transmission Electron Microscopy

Aliquots containing 2×10^7 cells were taken directly from suspension culture and added to an equal volume of HL5 with 6% glutaraldehyde. The cells were pelleted after a 3–5 min incubation, and resuspended in 5 ml of 3% glutaraldehyde, 0.2% tannic acid in 20 mM MOPS, 5 mM EGTA, 5 mM NaN_3, 5 mM $MgCl_2$, pH 6.8. After 10 min at room temperature, the cells were pelleted and washed one time in a large volume of the same buffer, then twice more in 0.1 M phosphate buffer, pH 6.8. All washes were done by resuspension of the cells and immediate centrifugation. The cells were postfixed for 20 min on ice in 1% OsO_4 in 0.1 M phosphate buffer, pH 6.0. After six washes in large volumes of ice-cold water, the cells were then en bloc stained in 2% uranyl acetate on ice for 30 min. The samples were then washed again in ice cold water as above, dehydrated through a graded series of ethanols, and embedded in Araldite in Eppendorf tubes. Only a portion of the cells were embedded as small pellets to permit complete infiltration.

Substrate-grown samples were prepared as previously described (Peterson et al., 1995), except cells were allowed to adhere to coverslips 24 h before fixation.

Scanning Electron Microscopy

Suspension-grown cells were permitted to adhere to Thermanox 25-mm round coverslips (Lux/Electron Microscopy Sciences, Fort Washington, PA) for 15 min in HL-5. The cells were then fixed in HL-5 with 3% glutaraldehyde, pH 6.8, for 10 min at room temperature, followed 20 min in the same glutaraldehyde-tannic acid fixative used for transmission EM. The samples were washed, postfixed, and dehydrated as described for transmission EM. The coverslips were dried in a Ladd critical point dryer, mounted on stubs, and sputter coated in a Hummer V sputter coater. The cells were examined on a Philips 501 and photographed on Polaroid Type 55 P/N film.

F-Actin Localization

Wild-type and mutant cells taken directly from suspension culture were allowed to adhere to a 22-mm coverslip for 15 min or 1 h in HL5. The F-actin distribution was determined by staining with rhodamine-phalloidin (Molecular Probes, Eugene, OR) and subsequent confocal microscopy as previously described (Peterson and Titus, 1994). Standard fluorescence microscopy was also used to collect a large number of images for quantification of cell size and crown size. Samples were examined with a Zeiss Axiophot using a 40× plan-neofluor objective, 1.3 N.A., and an optivar setting of 1.25. The fluorescence images were collected with a Photometrics Star 1 camera system (Photometrics Ltd.) and analyzed with IP Lab software (Signal Analytics Corp., Vienna, VA).

The distribution of crowns on each cell type was determined by examining the rhodamine-phalloidin–stained cells. Each field was photographed at a sufficient number of focal planes to capture all of the brightly staining, circular or ovoid projections. Images of cells at their base were also collected, and measured along their longest axis and on an axis roughly perpendicular to this (approximate length and width). These dimensions were used to calculate an approximate cell area. An average width was used for oddly shaped cells. The curvature of the smaller cells (<470 μm^2 in apparent area) made definitive measurements of cell surface area difficult due to the likelihood of underestimating the true area. Images of all three cell types were examined and cells empirically determined to be well-spread by general morphological comparison (the number of focal planes, shape of the cell, etc. were examined). The lowest calculated area of cells in this subclass was 470 μm^2. Therefore, all of the comparisons were made on cells that had an apparent area of ≥470 μm^2.

Double Staining for F-Actin and myoB

1×10^6 KAx3 and *myoB*$^-$ cells were taken from suspension and allowed to adhere to coverslips 10 min. They were immediately fixed in acetone for 10 min at −15°C. Coverslips were then washed 3×5 min in PBS and incubated with preabsorbed myoB antibody (M. A. Titus, unpublished data) for 30 min at 37°C. The myoB antibody was generated against the myoB tail region and preabsorbed using fixed cells (Fukui et al., 1987). The preabsorbed antibody reacts with a single band of ~130 kD in blots of KAx3 cells, and did not cross-react with any other of the *Dictyostelium* myosin Is based on the lack of the 130-kD band in extracts of *myoB*$^-$ cells. Coverslips were washed again 3×5 min in PBS, and incubated with Cy5 donkey anti–rabbit antibody for 30 min at 37°C (Jackson Immunochemicals, West

Grove, PA). After three more washes in PBS, cells were stained with rhodamine-phalloidin and examined by confocal microscopy as previously described (Peterson and Titus, 1994).

Miscellaneous

The development of *Dictyostelium* was performed as previously described (Peterson et al., 1995). Unless otherwise stated, reagents were purchased from Sigma; restriction enzymes were obtained either from New England Biolabs (Beverly, MA) or Boehringer Mannheim Corp. (Indianapolis, IN).

Results

Generation of Dictyostelium Myosin I Double Mutants

Two *Dictyostelium* myosin I double mutant strains were created by disrupting the *myoB* gene in either the *myoA*$^-$ or *myoC*$^-$ single mutant strains (Peterson et al., 1995), using neomycin drug resistance as a selectable marker. Homologous recombination of one copy of the gene replacement fragment at the *myoB* target locus resulted in a loss of 2.2 kb of the *myoB* gene contained between, and including, the two BclI sites. Southern blotting confirmed that a 1.1-kb HindIII/EcoRI probe from the 3′ end of the *myoB* gene hybridized to a 1.4-kb band in EcoRI/BclI-digested KAx3 (wild type) DNA and a 5.4-kb band in EcoRI/BclI-digested double mutant DNA (Fig. 1 *A*). The loss of the two internal BclI sites observed in the Southern analysis is consistent with the replacement of the internal 2.2 kb BclI fragment by the 2.1-kb Neo cassette. Two independent transformation experiments were carried out, 20 colonies were screened for each, and 8–10 clones proved to be homologous recombinants for each transformation. A single clone from each round of transformation was used for all subsequent analysis. The two independent clones for each double mutant were analyzed in detail, and the combined results are presented below.

Recombination of the selection marker into the targeted myosin I gene loci resulted in lack of full-length mRNA from the disrupted gene. A Northern blot of poly(A)$^+$-selected RNA from wild-type and double mutant cell lines that had been allowed to develop for 3 h was probed sequentially with fragments from each of the three myosin I genes (Fig. 1 *B*). The *myoA* probe hybridized with an ~3.5-kb full-length mRNA transcript from KAx3 cells. This 3.5-kb *myoA* transcript was absent in the *myoA*$^-$/*B*$^-$ strain, but was still present in the *myoB*$^-$/*C*$^-$ strain (Fig. 1 *B*). The *myoB* probe hybridized to a slightly larger transcript of ~3.8 kb in the KAx3 strain that was undetectable in either the mRNA from *myoB*$^-$/*C*$^-$ or *myoA*$^-$/*B*$^-$ cells. The *myoC* probe hybridized with a 4.0-kb transcript in KAx3 RNA that was absent from the *myoB*$^-$/*C*$^-$ cells, but still detectable in the *myoA*$^-$/*B*$^-$ cells (Fig. 1 *B*). It is highly unlikely that any functional protein is produced in the mutant strains as the predicted remaining region of each of the myosin heads would contain only the nucleotide-binding P-loop and lack the actin binding site.

Myosin I Double Mutants Exhibit Slow Rates of Pinocytosis

The most striking defect observed in both myosin I double mutants is a decreased rate of pinocytosis. The fluid phase marker FITC-dextran was used to measure pinocytosis

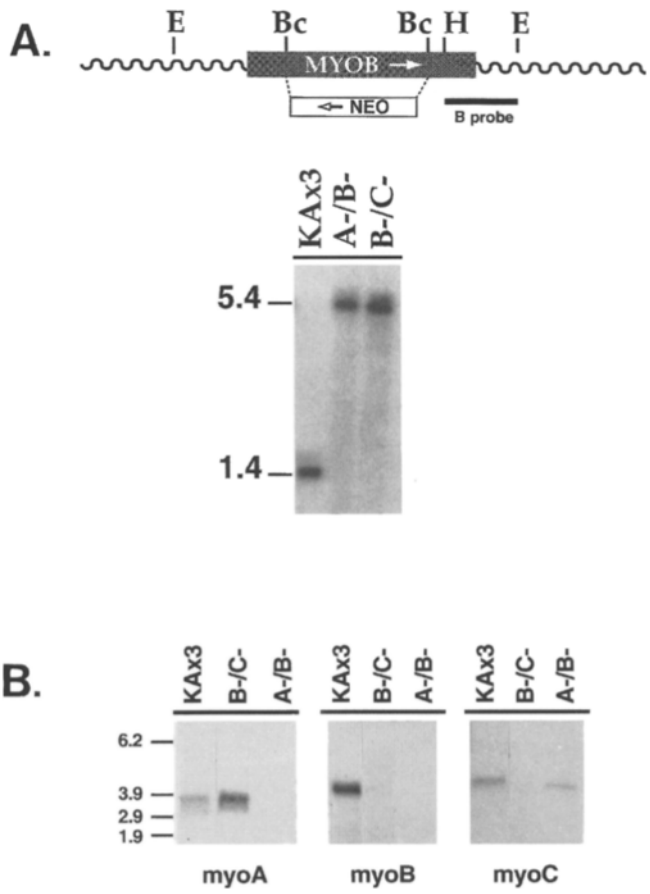

Figure 1. Southern and Northern blot analysis demonstrates that the *myoB* gene is disrupted in the *myoA*$^-$ and *myoC*$^-$ strains. (*A*) Southern analysis of the *myoB* locus. Shown at the top is a schematic diagram of the *myoB* locus. The wavy lines indicate the extragenic regions, the dark box the individual locus, the small solid black rectangle labeled probe indicates the region used for a probe, and the open box (marked NEO) connected to the gray box indicates the region where the selectable marker was inserted. *NEO*, neomycin transferase gene; *E*, EcoRI; *Bc*, BclI; *H*, HindIII. The bottom half of the panel is the Southern blot. A 1.1-kb probe derived from the 3′ end of the gene (see Materials and Methods) detects a 1.4-kb fragment in wild-type cells (KAx3). Insertion of the neomycin resistance gene into *myo*B locus of either the *myoA*$^-$ or *myoC*$^-$ strain results in the deletion of the two BclI sites and increases the size of the detected fragment to 5.4 kb (*myoA*$^-$/*B*$^-$ and *myoB*$^-$/*C*$^-$, respectively). The molecular mass of each band is indicated on the left, in kb. A total of 20 μg of genomic DNA from each strain was digested with EcoRI and BclI, subjected to electrophoresis on an 0.8% agarose gel and transferred to nylon. The hybridization and washes were carried out using Quik-Hyb (Stratagene, La Jolla, CA) following the instructions provided by the manufacturer. (*B*) Northern analysis of the myosin I double mutants. Poly(A)$^+$ RNA was isolated from wild-type (KAx3) and double mutant cell lines (*myoB*$^-$/*C*$^-$, *myoA*$^-$/*B*$^-$) after 3 h in starvation buffer. Equal amounts of the poly(A)$^+$ RNA were loaded on formaldehyde gels, subjected to electrophoresis, and transferred to nylon membrane. The blots were probed with the DNA probes derived from the *myo* genes (see Materials and Methods) indicated at the bottom of the figure. The numbers to the left of the blot indicate the positions of RNA size markers, in kb.

(Klein and Satre, 1986) in wild-type, single mutant, and double mutant strains (Fig. 2 *A*). When cells were grown and assayed for pinocytosis in suspension, wild-type (KAx3), JH10, and myosin I single mutants steadily accumulated ~0.8–0.9 μl FITC-dextran/10^6 cells over the course of 1 h (Fig. 2 *A*). The KAx3 cells reached a fluid internalization plateau of 1.1 μl/10^6 cells after 2 h (Fig. 2 *A*). The *myoA*$^-$/*B*$^-$ and *myoB*$^-$/C$^-$ cells, however, internalized FITC-dextran at a slower rate. They accumulated 0.3 μl FITC-dextran/10^6 cells by 60 min, a decrease of ~60%, and reached a fluid internalization plateau of 0.45 μl/10^6 cells after 1.5 h (Fig. 2 *A*). The endocytic defect observed in the double mutants was not simply due to the presence of G418 in the medium. A control neomycin-resistant cell line did not exhibit pinocytic defects in the presence of G418 when placed in suspension (data not shown).

Interestingly, when substrate-grown cells were assayed for pinocytosis while still attached, the double mutant cells steadily accumulated FITC-dextran at rates similar to KAx3 and myosin I single mutants over the course of 1 h (Fig. 2 *B*). All of the strains accumulated a total of ~0.5–0.6 μl FITC-dextran/10^6 cells under these conditions. When maintained on a substrate, the double mutants internalize almost twice the volume as in suspension over the course of 1 h (compare Fig. 2 *A* with *B*).

The endocytic defect observed in both myosin I double mutants is not the result of a general disruption of cell function due to maintenance in suspension culture. The endocytic defect is immediate: when either of the double mutant cells are transferred from a substrate to suspension culture, and endocytic activity measured after 1 h in suspension, a significant decrease relative to wild-type uptake is observed (Fig. 2 *C*). The mutants internalize 0.27 μl FITC-dextran/10^6 cells, versus 0.85 μl for the wild-type cells (Fig. 2 *C*), an amount similar to that observed for cells previously carried in suspension for 72 h (compare with Fig. 2 *A*). Conversely, when suspension-grown cells are placed on a substrate for 45 min, they regain the ability to pinocytose at an increased rate, taking in 0.5 μl FITC-dextran/10^6 cells after 1 h, an amount comparable to that internalized by the wild-type cells (Fig. 2 *D*).

The internalization of solid particles by the double mutants in suspension was evaluated using a bacterial clearing assay. The ability of the myosin I double mutants to clear a bacterial culture over a 5 h time period was observed. All cell lines internalized bacteria steadily throughout the time course (Fig. 3). The *myoA*$^-$ and *myoC*$^-$ single mutants (Fig. 3, *open triangles* and *open circles*) did not differ substantially from wild-type (Fig. 3, *Xs*, *dashed line*) in their ability to clear the bacterial suspension, indicating that these single mutants had normal phagocytic activity. A slight slowing in the decrease of optical density was observed in suspensions containing the *myoB*$^-$ single mutant (Fig. 3, *open squares*), consistent with previous reports (Jung and Hammer, 1990). A similar decrease was seen in the *myoB*$^-$/*C*$^-$ double mutant (Fig. 3, *filled circles*). The *myoA*$^-$/*B*$^-$ mutant did not, however, exhibit decreased phagocytic activity in any of the three trials (Fig. 3, *filled triangles*). These findings support previous studies suggesting that phagocytosis and pinocytosis occur via distinct mechanisms (Bacon et al., 1994; Cohen et al., 1994).

The pinocytic defect was further illustrated by fluorescence microscopy of suspension-grown cells following a 1-h incubation with FITC-dextran (Fig. 4). The double mutant cells appear to have internalized less FITC-dextran than the wild-type cells, and fewer fluorescent vesicles were ob-

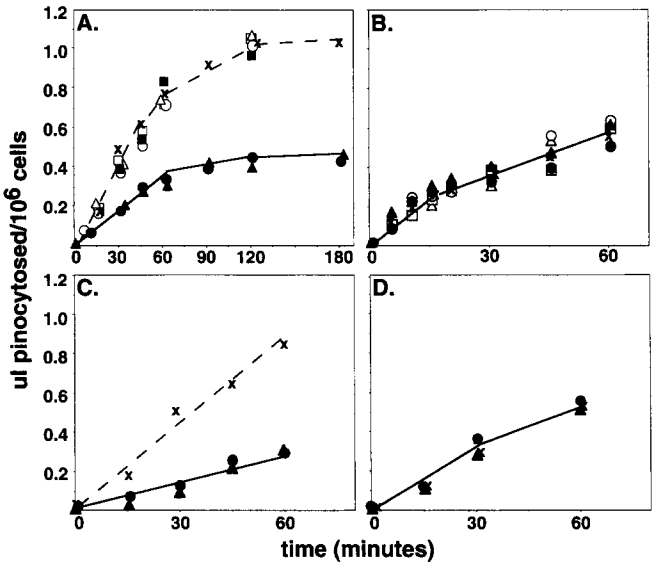

Figure 2. The double mutant cells exhibit a conditional pinocytic defect. (*A*) The uptake of FITC-dextran by each of the suspension-grown strains. (*B*) Uptake of FITC-dextran by each of the cell lines maintained and assayed on a substrate. (*C*) Uptake of FITC-dextran by cells grown on a substrate but assayed after 1 h in suspension. (*D*) cells from suspension culture that have been permitted to adhere to a substrate for 45 min before the assay. (*A–D*) KAx3 (X); JH10 (■); *myoA*$^-$ (△); *myoB*$^-$ (□); *myoC*$^-$ (○); *myoA*$^-$/*B*$^-$ (▲); *myoB*$^-$/*C*$^-$ (●). Points shown are the average of at least three experiments.

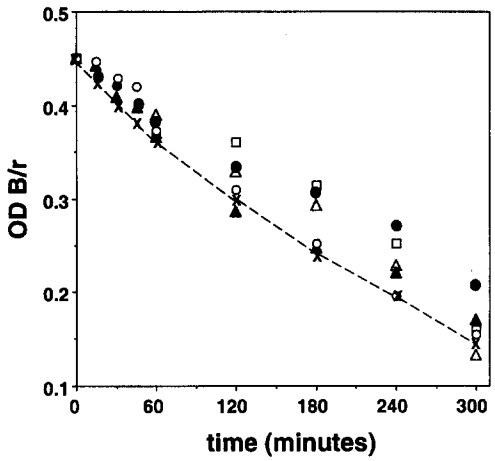

Figure 3. Myosin I double mutants undergo normal phagocytosis of bacteria. Wild-type KAx3 cells (*X*); *myoA*$^-$ (△); *myoB*$^-$ (□); and *myoC*$^-$ (○) single mutant cells; and *myoA*$^-$/*B*$^-$ (▲); and *myoB*$^-$/*C*$^-$ (●); cells were inoculated into suspension cultures of *E. coli* B/r of OD_{600} = 0.45. The ability of each of the different cell lines to clear the bacterial culture was measured by the decrease in optical density of the bacteria over the course of 5 h.

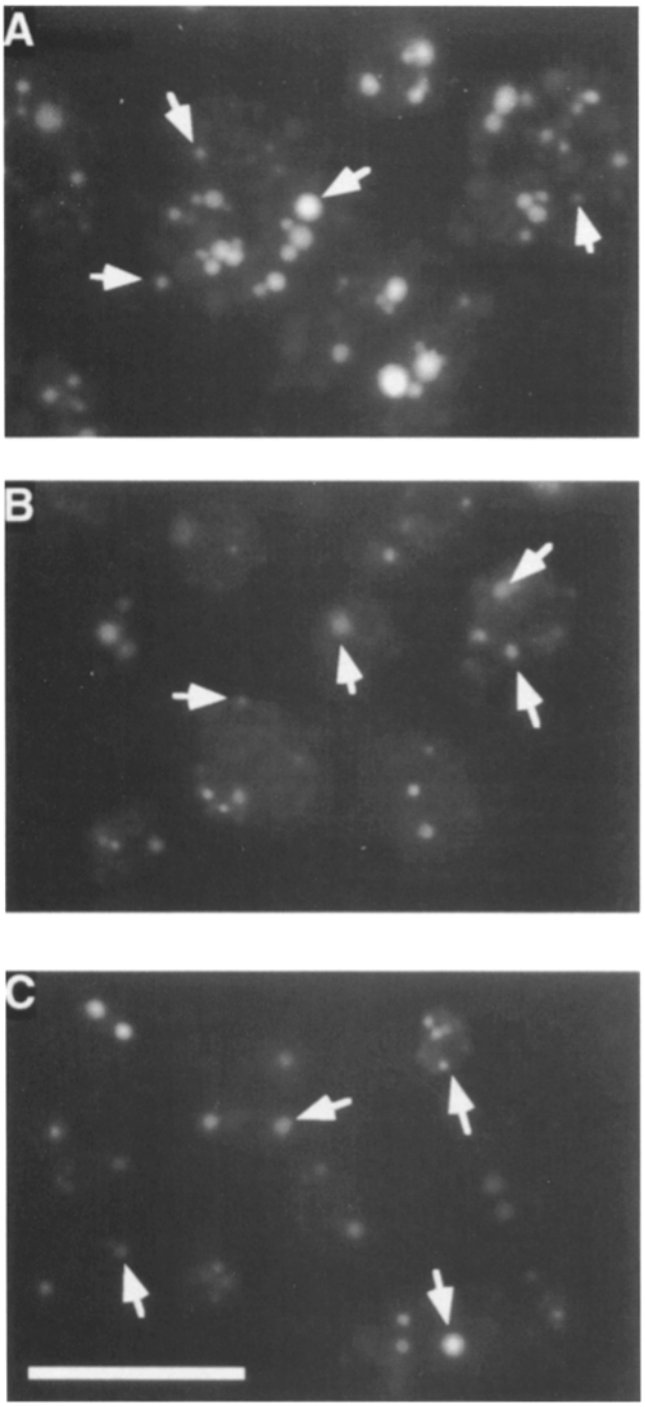

Figure 4. The suspension-grown myosin I double mutants contain fewer endocytic vesicles. Fluorescent images of suspension-grown KAx3 (*A*), *myoA*$^-$/*B*$^-$ (*B*), and *myoB*$^-$/*C*$^-$ (*C*) after 60-min incubation in FITC-dextran illustrate the reduced level of pinocytic activity of the double mutant cells. Arrows indicate examples of fluorescent vesicles counted. Bar, 10 μm.

Table I. Growth of Myosin I Mutants in Suspension Versus on a Substrate

Cell Line	Substrate doubling time	Suspension doubling time	Susp. sat. density
	h	*h*	*cells/ml*
KAx3	13	9	1×10^7
JH10	13	9	1×10^7
G418 control	13	9	1×10^7
myoA$^-$	13.5	11	1×10^7
myoB$^-$	13.8	10.5	1×10^7
myoC$^-$	13.6	10	1×10^7
myoA$^-$/*B*$^-$	17.1	24	2.5×10^6
myoB$^-$/*C*$^-$	16.8	22	2.5×10^6

Shown are the average doubling times (n = 3) for each cell line, KAx3 is the parental wild-type strain and control is a G418 resistant nonhomologous recombinant. The density of cells grown either in suspension or on a substrate was determined every 24 h over a 7–10-d period, and the doubling time obtained from growth rates that occurred during log phase growth.

served (compare Fig. 4 *A* with *B* and *C*). The number of fluorescent vesicles per cell was determined. The KAx3 cells contained an average of 15.4 fluorescent vesicles per cell (SD = 6.1; n = 40), while *myoA*$^-$/*B* cells contained only an average of 4.8 fluorescent vesicles per cell (SD = 2.5; n = 61), and the *myoB*$^-$/*C*$^-$ cells only contained an average of 3.5 fluorescent vesicles per cell (SD = 2.3; n = 100).

The ability of *Dictyostelium* strains to grow axenically in liquid culture correlates with their pinocytic activity (Maeda and Kawamoto, 1986). The observed difference between rates of pinocytosis in suspension versus on a substrate parallels growth rates of the various strains under the two conditions (Table I). The doubling time of KAx3, JH10, the G418 resistant control, and single mutant cell lines in suspension cultures was 9–11 h at log phase, and all four strains saturated growth at the normal density, 1×10^7 cells/ml (Table I). In contrast, both double mutants growing in suspension exhibited a doubling time of 22–24 h at log phase and saturated growth at a lower cell density, 2.5 x 10^6 cells/ml. The decreased growth rate observed for the double mutants was similar to that observed for KAx3 cells in diluted growth medium. KAx3 cells grown in half-strength HL5 also have an increased doubling time, 22 h, and saturate at a lower density, 4.5×10^6 cells/ml, than when placed in normal medium (data not shown). The defect of cell growth in the double mutants was not simply due to the presence of G418 in the medium. The neomycin-resistant control cells did not show growth rate defects in the presence of G418 (Table I).

Growth of the myosin I double mutants was closer to wild-type rates when cells were transferred from suspension culture to a substrate. They initiate log phase growth within 48 h, and proceed to double in cell number approximately every 16–17 h. The KAx3 and myosin I single mu-

Figure 5. Ultrastructural analysis of suspension-grown double mutants reveals an abnormal vesicle profile in double mutant cells. The KAx3 (*A* and *B*), *myoA*$^-$/*B*$^-$ (*C* and *D*), and *myoB*$^-$/*myoC*$^-$ (*E* and *F*) were grown and fixed while in suspension and processed for thin sectioning electron microscopy. A representative gallery of images is shown. Note the reduced number of large, clear vesicles in the mutant cell lines. The double mutants also possess many small, debris-filled vesicles. Examples of the large, clear vacuoles are indicated with arrowheads, while representative contractile vacuoles are marked with arrows. Bar, 2 μm.

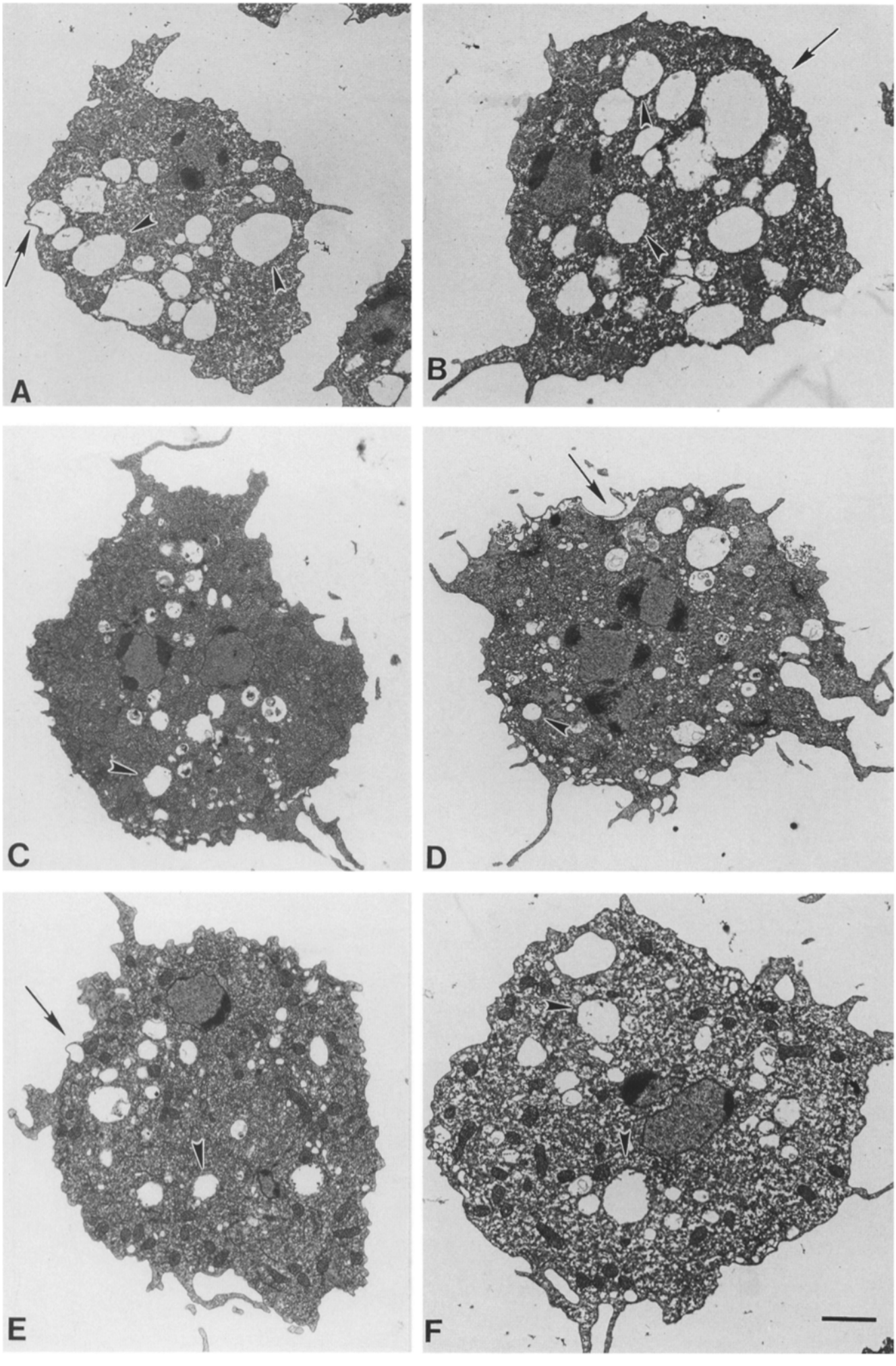
A
B
C
D
E
F

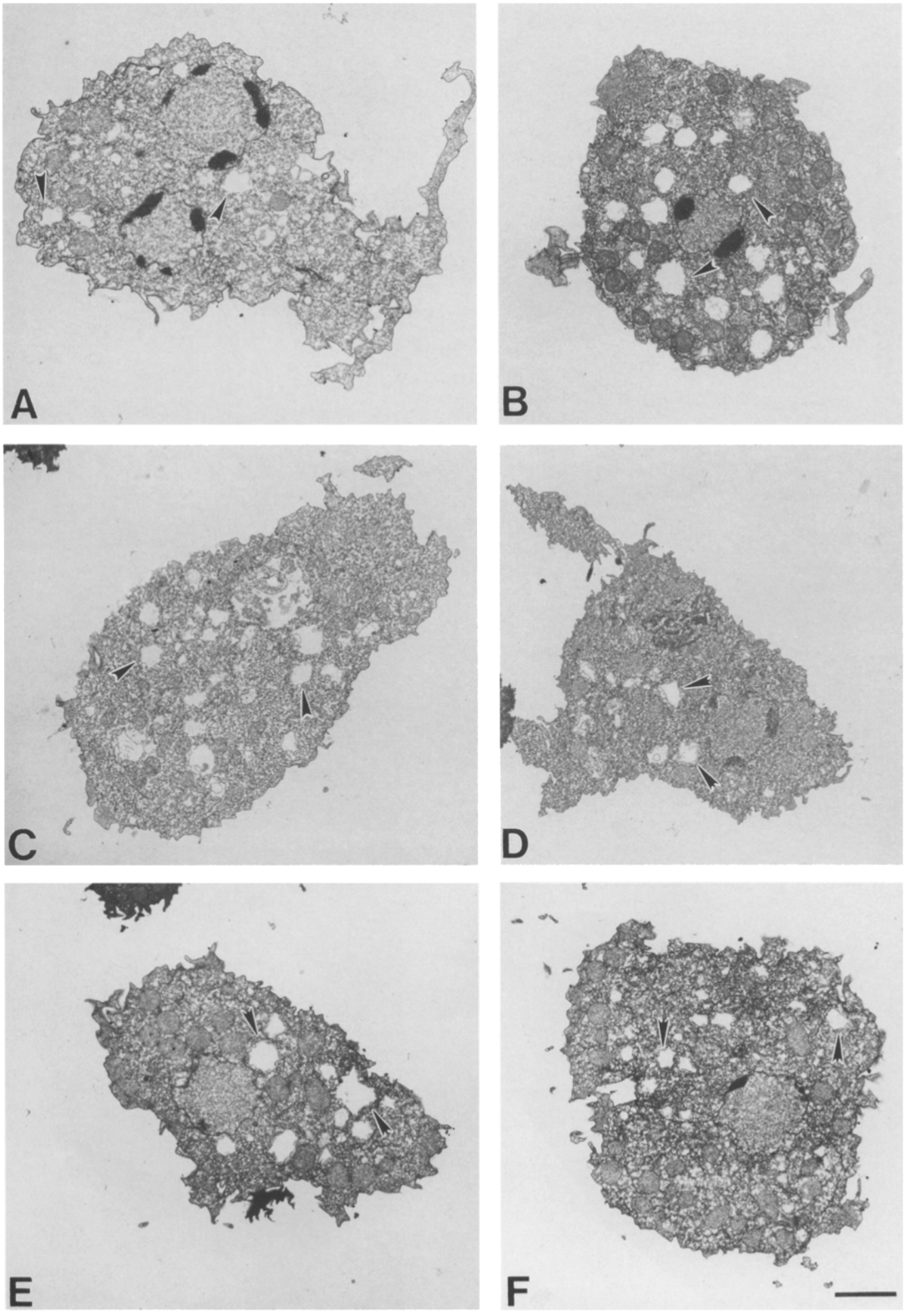
A
B
C
D
E
F

tant strains initiated log phase growth within 24 h of being placed on a substrate, and doubled in cell number every 13 h.

Suspension-grown Myosin I Double Mutants Exhibit an Altered Vesicle Profile

Ultrastructural analysis was undertaken to determine if the endocytic defect uncovered by the FITC-dextran uptake assay and images was reflected in the internal morphology of the suspension-grown double mutants. The KAx3 and *myoA*$^-$/*B*$^-$ and *myoB*$^-$/*myoC*$^-$ double mutant strains were each fixed and processed for electron microscopy entirely in suspension. The KAx3 cells exhibited a typical complement of vesicles and vacuoles. The most obvious of these were many large, empty compartments thought to be associated with the endocytic pathway. Other vesicles observed included digestive vesicles, that contain cellular debris, and contractile vacuoles. Contractile vacuoles were identified as large clear or collapsed vesicles with a very thin strip of cytoplasm between the vesicle and the plasma membrane. Tubular elements extending from contractile vacuoles appear as clusters of small vesicles in thin section (see Fig. 5 *E*). This overall morphology has been previously observed in other axenic strains (Ryter and deChastellier, 1977; Zhu and Clarke, 1992). The TEM morphologies of the suspension-grown myosin I single mutants (*myoA*$^-$, *myoB*$^-$, and *myoC*$^-$) were identical to that of KAx3 cells (data not shown).

The *myoA*$^-$/*myoB*$^-$ double mutant exhibited a distinctly different internal vesicle profile from KAx3 (Fig. 5, *C* and *D*). These cells contained numerous small vesicles, while large clear vesicles were rarely observed. This result is consistent with the reduced number of FITC-dextran filled endocytic vesicles observed by fluorescent microscopy (Fig. 4). Most of the intermediate-sized vacuoles appeared to contain debris, unlike those of the wild type. The *myoA*$^-$/*B*$^-$ cells also appeared to have more projections emanating from the cell surface (Fig. 5, *C* and *D*). The *myoB*$^-$/*C*$^-$ were similar to the *myoA*$^-$/*B*$^-$ cells in that they did not appear to contain the same proportion of large vacuoles as wild type cells (Fig. 5, *E* and *F*). Contractile vacuole structures in the double mutants were identical to those observed in our wild-type KAx3 strain and previously published micrographs (Ryter and deChastellier, 1977; Zhu and Clarke, 1992). Staining of these cells with an anti-calmodulin antibody (Hulen et al., 1991) also demonstrated that the contractile vacuole structure is similar between wild-type and double mutant cells (Temesvari et al., manuscript submitted for publication).

Based on the observation that myosin I double mutants undergo fluid-phase pinocytosis at the same rate as KAx3 cells when attached to a substrate, we observed the internal morphology of cells maintained under these conditions. Substrate-grown KAx3 (Fig. 6, *A* and *B*) and double mutant cells (Fig. 6, *C–F*) each contain many large empty vacuoles, as well as contractile vacuoles. No difference in vesicle size or internal morphology is apparent between wild-type and double mutant cells maintained on a substrate. The average size of vesicles does, however, appear to be smaller in substrate-grown KAx3 vs. suspension-grown KAx3 cells (compare Fig. 5, *A* and *B* with Fig. 6, *A* and *B*).

Internalization of a Cell Surface Protein is Defective in Myosin I Double Mutants

The defect in endocytosis, along with the altered vesicular profiles, suggested that the myosin I double mutants may be compromised during the early vesicle internalization step of endocytosis. We examined membrane internalization in these cells by following uptake of gp126, a 116-kD cell surface protein that is internalized by cells at room temperature (Bacon et al., 1994). *Dictyostelium* cell surface proteins were labeled by glutathione-cleavable biotinylation (Goodloe-Holland and Luna, 1987). A number of cell surface proteins were labeled in the biotinylated, unstripped samples (Fig. 7, *U lanes*). The gp126 became internalized and protected from glutathione cleavage after 10-min incubation, and its accumulation continued for up to 1 h (Fig. 7, KAx3).

Internalization of gp126 was delayed and decreased in the suspension-grown myosin I double mutants. (Fig. 7, compare the 116-kD band in the KAx3 versus A$^-$/B$^-$ and B$^-$/C$^-$ lanes). The band corresponding to gp126 was visible by 10 min in the *myoA*$^-$/*B*$^-$ mutants, but at a much lower intensity than that of KAx3 (compare Fig. 7 *KAx3* with *A*$^-$/*B*$^-$). There was a steady accumulation of gp126 in the *myoA*$^-$/*B*$^-$ sample over the course of the hour, but wild-type levels were not attained. The *myoB*$^-$/*C*$^-$ mutants also internalized gp126, but at much lower levels than KAx3 (Fig. 7, *B*$^-$/*C*$^-$). The rate of internalization of gp126 in the *myoA*$^-$, *myoB*$^-$, and *myoC*$^-$ single mutant strains as well as in the double mutant cells attached to a substrate was indistinguishable from that of the wild-type KAx3 strain (data not shown).

Suspension-grown Double Mutants Exhibit More Cell Surface Projections and Rearrange Their F-actin Cytoskeleton Less Efficiently Than KAx3 Cells

The TEM observation that the double mutants appeared to extend more cell surface projections, and correlations made between membrane projections and fluid uptake in mammalian cells (Dowrick et al., 1993) led us to examine the surface of these cells by scanning electron microscopy and rhodamine-phalloidin staining. The suspension-grown double mutants were allowed to adhere to a substrate for a short time, 15 min, before fixation and processing for SEM. More numerous protrusions, both crowns (de Hos-

Figure 6. Ultrastructural analysis of substrate grown double mutants reveals that they are similar to KAx3. The KAx3 (*A* and *B*), *myoA*$^-$/*B*$^-$ (*C* and *D*), and *myoB*$^-$/*myoC*$^-$ (*E* and *F*) were grown and fixed while attached to a surface for thin sectioning electron microscopy. The distribution of large, clear endocytic vesicles (marked with arrow heads) is similar between KAx3 and double mutant cells. Bar, 2 μm.

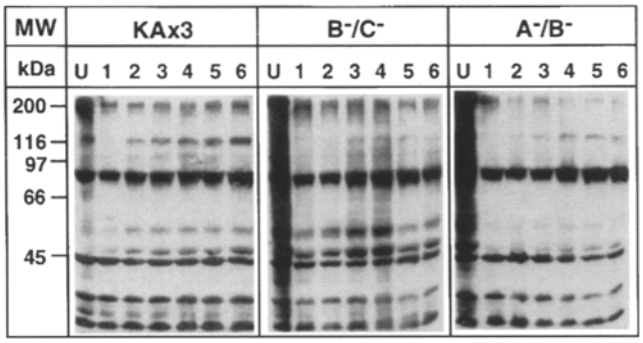

Figure 7. Myosin I double mutants are defective in membrane uptake. Cell surface proteins of wild-type (*KAX3*), *myoB*$^-$/*C*$^-$ (*B*$^-$/*C*$^-$), and *myoA*$^-$/*B*$^-$ (*A*$^-$/*B*$^-$) strains were labeled with a cleavable biotin analogue at 0°C. The cells were allowed to internalize labeled protein at 24°C for 0 (*1*), 10 (*2*), 20 (*3*), 30 (*4*), 45 (*5*), and 60 (*6*) min, returned to ice, and remaining cell surface biotin was stripped with glutathione. Internalized proteins were visualized by immunoblotting using streptavidin-HRP and chemiluminescence. An equal amount of sample was loaded in each lane. The control unstripped biotinylated cells (*U*) are shown for comparison. A 70-kD band present in all lanes is an endogenous biotin-containing protein. Molecular mass is indicated to the right, in kD. The arrow on the right side indicates the position of the 116-kD band that is protected from the stripping as internalization time increases.

tos et al., 1991) and filopodia, cover the dorsal surfaces of the double mutants and are readily apparent when the images are compared with those of wild-type cells (Fig. 8). The double mutants also appeared to be smaller and rounder than the wild-type cells (compare Fig. 8, *A* with *B* and *C*). However, cell remnants were observed on the coverslips of the SEM samples. This suggested that there was a loss of larger, flattened cells during the processing the cells are subjected to for SEM. The presence of large, apparently flat cells in the images of rhodamine-phalloidin stained cells after 15 min adherence was consistent with this observation (Fig. 9, *C–F*). These results suggested that the double mutant cells tend to attach less strongly to plastic than the KAx3 cells. The loss of the larger cells and the curvature of the remaining cells made a quantitative comparison of the cell area and number of crowns in the SEM samples difficult due to the likely underestimation in both measurements.

The double mutants were also subjected to rhodamine-phalloidin staining to fully evaluate the number and distribution of the surface projections, which are known to contain significant amounts of F-actin. The F-actin organization in the KAx3 and myosin I single mutant cells, as well as aggregation-competent double mutant cells, during attachment to a substrate has been described previously (Fukui et al., 1991; Peterson and Titus, 1994; Peterson et al., 1995). The F-actin staining at the base of suspension-grown wild type cells that were allowed to adhere to a substrate for 15 min appeared as bright, thick bands or rings of stain that usually corresponded to regions of membrane extension (Fig. 9 *A*). Diffuse cytoplasmic staining was also noted. A thin line defined the periphery of these well-

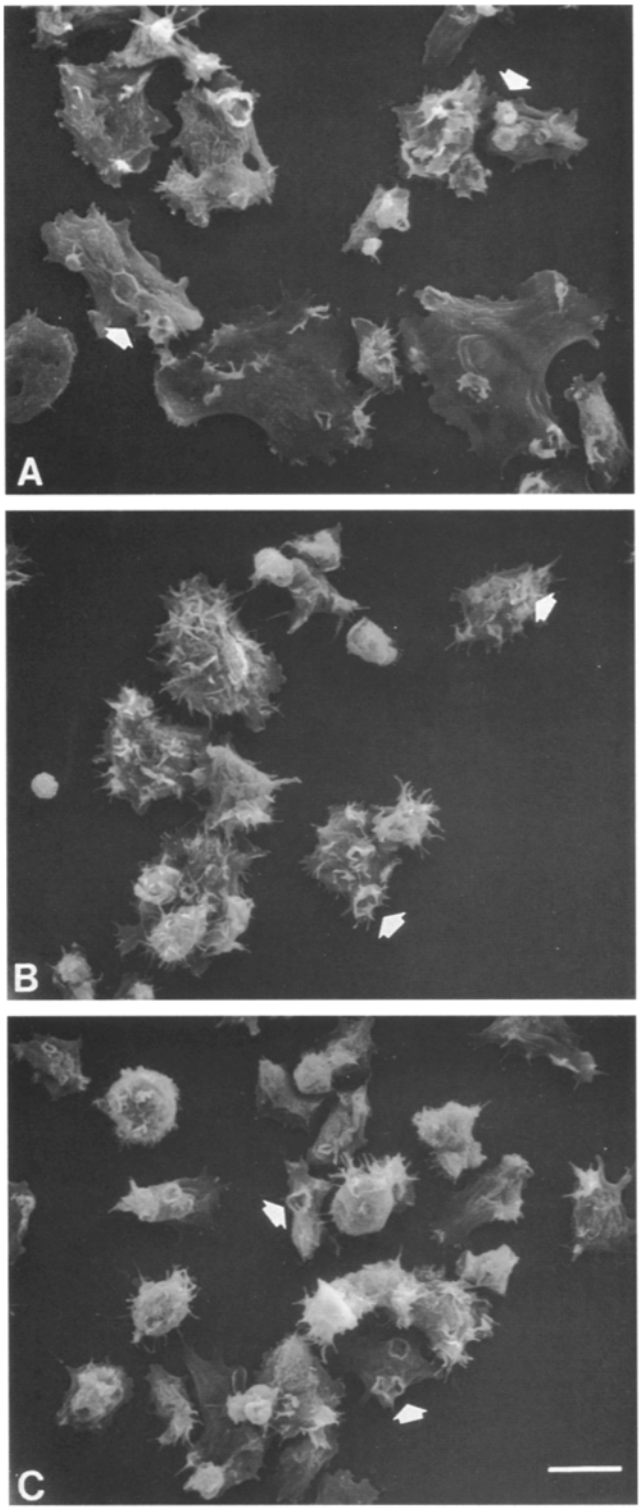

Figure 8. Myosin I double mutants appear to extend more protrusions from the cell surface. The KAx3 (*A*), *myoA*$^-$/*B*$^-$ (*B*), and *myoB*$^-$/*C*$^-$ (*C*) strains were taken from suspension culture, allowed to adhere to a coverslip in nutrient medium for 15 min, fixed, and then processed for scanning electron microscopy. Examples of the crowns or circular ruffles are marked with arrows. The flatter KAx3 cells (*A* and *B*) have fewer spiky filopodia than the *myoA*$^-$/*B*$^-$ (*B*) or *myoB*$^-$/*C*$^-$ (*C*) cells. Bar, 10 μm.

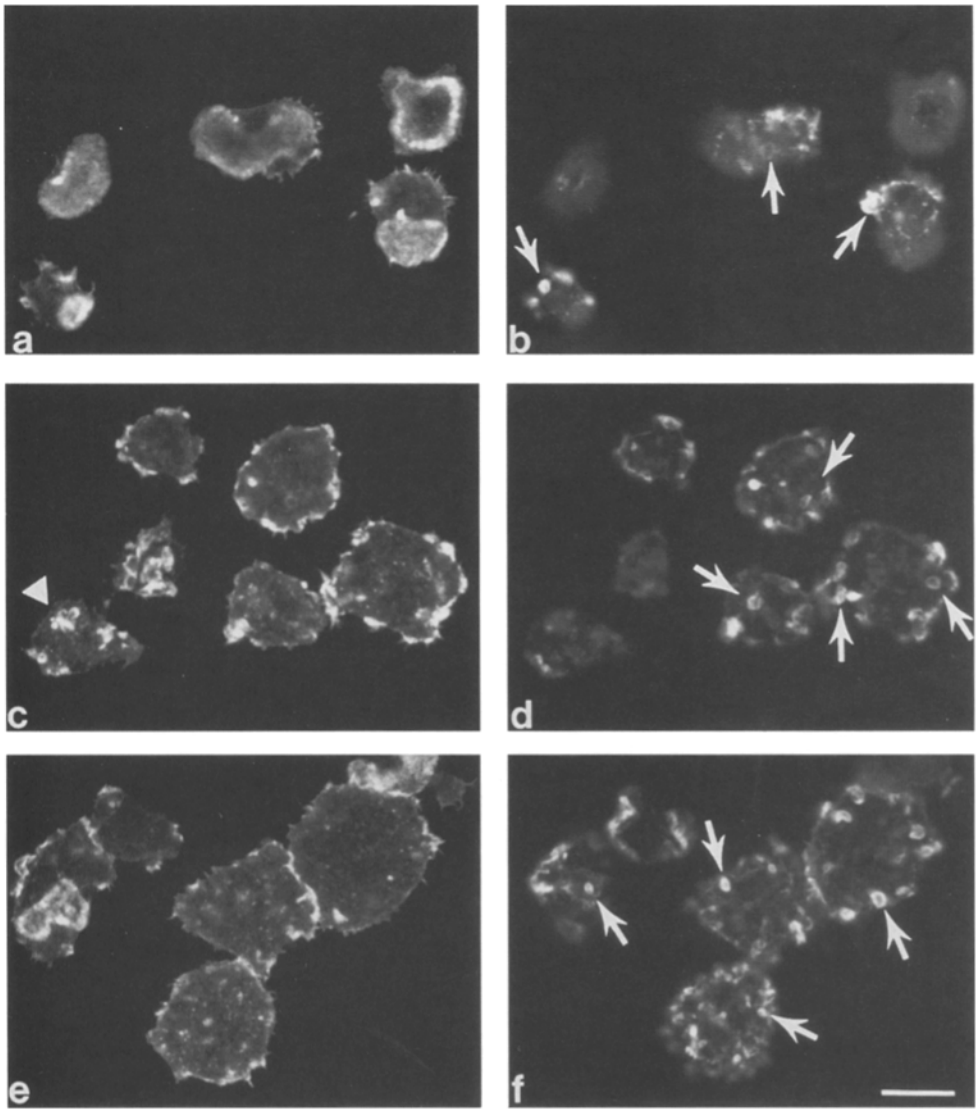

Figure 9. The myosin I double mutants exhibit distinct patterns of F-actin staining. The KAx3 (*A* and *B*), *myoA*$^-$/*B*$^-$ (*C* and *D*) and *myoB*$^-$/*C*$^-$ (*E* and *F*) strains were taken from suspension culture, allowed to adhere to a coverslip in nutrient medium for 15 min, fixed, and then processed for rhodamine-phalloidin staining. Shown are confocal images of the bottom (*A*, *C*, and *E*) and top (*B*, *D*, and *F*) surface of several cells. Examples of crowns are indicated with arrows; the triangle in *C* marks a cluster of small crowns. Bar, 10 μm.

spread cells, and filopodia were stained (Fig. 9 *A*). The dorsal surfaces of the wild-type cells had a few, small brightly staining projections (Fig. 9 *B*).

The suspension-grown myosin I double mutants exhibited different patterns of F-actin staining during attachment to a surface. The majority of cells concentrated actin in small pseudopodia, filopodia, foci, and around the periphery of the cell (Fig. 9, *C* and *E*). The thick bands or rings of stain characteristic of the wild-type cells were present in only a few of the double mutant cells (data not shown). The double mutants had numerous brightly staining circular rings or projections on their dorsal surfaces (Fig. 9, *D* and *F*). These structures correspond to "crowns" and amoebastomes, which are frequently observed in both protozoan and mammalian cells (de Hostos et al., 1991; Dowrick et al., 1993). Such structures are believed to be phagocytic in *Acanthamoeba* and macropinocytotic in mammalian cells. Their exact function in *Dictyostelium* is unknown.

Quantification of the number of these crowns per cell in well-spread cells (cells that were ≥470 μm^2 in estimated area, had few focal planes, and appeared to be spread based on their overall shape) indicated that both double mutants appear to possess more numerous crowns than the wild-type cells (Table II). Both of the double mutants were found to make, on average, at least two times more crowns per unit area (Table II). The double mutant cells

Table II. Analysis of Crowns Formed by the Myosin I Double Mutants

Strain	No. cells	No. crowns	Crown per cell	Cell Area	μm^2 of cell area per crown
				μm^2	
KAx3	31	151	4.9	736.1 ± 43.5	150.2
myoA$^-$/*B*$^-$	31	302	9.7	818.3 ± 67.0	84.4
myoB$^-$/*C*$^-$	31	358	11.5	786.1 ± 40.6	68.4

Cells were taken from suspension and allowed to adhere to the coverslip for 15 min before processing for visualization of crown structures by rhodamine-phalloidin fluorescence. Shown are the number of cells and crowns counted in cells with an area of ≥470 mm^2, the mean cell area (±SE) for each cell type is also presented. These values were used to calculate the μm^2 of cell area per crown (μm^2 per cell/crowns per cell).

eventually redistributed their F-actin in a pattern resembling wild-type cells following longer adhesion times, but never fully achieved a wild-type distribution (data not shown; Peterson and Titus, 1994).

Myosin I Is Localized to F-actin Filled Projections in Vegetative Cells

The potential role of one of the *Dictyostelium* myosin Is, myoB, in control of crown formation was evaluated by carrying out immunofluorescence localization in cells adhering to a substrate. KAx3 cells taken from suspension cultures were double stained for F-actin and myoB, and observed by confocal microscopy. The myoB staining in these cells was mostly of a diffusely cytoplasmic nature, but foci of myoB were observed at the plasma membrane, with a patchy association of myoB with the F-actin stained crown structures (compare Fig. 10, *C* with *D*). This localization is not as distinct as for F-actin, and not all crown structures contained myoB. MyoB null cells, which exhibited F-actin staining patterns identical to wild-type (Fig. 10 *A*), did not stain for myoB (Fig. 10 *B*). This myoB staining

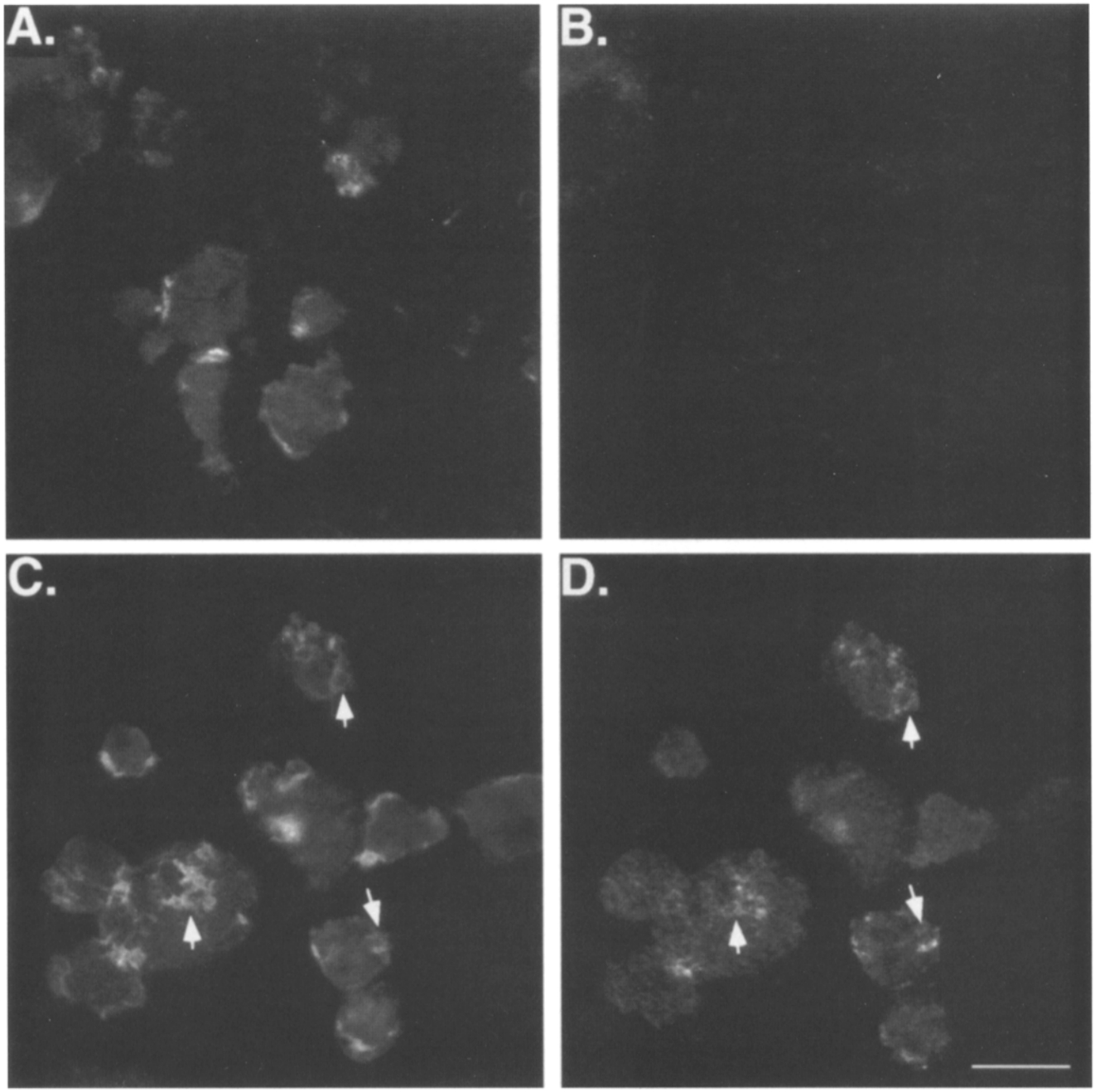

Figure 10. Myosin I colocalizes with F-actin to membrane extensions in vegetative KAx3. *myoB*$^-$ (*A* and *B*) and KAx3 cells were taken from suspension culture, allowed to adhere to a coverslip for 10 min, fixed, and processed for both rhodamine-phalloidin staining (*A* and *C*) and myoB immunofluorescence (*B* and *D*). All views are confocal images viewed from the top surface of cells. Examples of crowns that contained myoB are marked with arrows. Bar, 10 μm.

pattern differs from that observed in KAx3 cells undergoing chemotaxis (Fukui et al., 1989).

Motility and Development of the Myosin I Double Mutants

The finding that the *myoA*$^-$ and *myoB*$^-$ cells were less efficient in cellular translocation suggested that the *myoA*$^-$/*B*$^-$ mutants may be further impaired. The instantaneous velocity of aggregation-competent myosin I double mutants grown in suspension was measured as described previously (Peterson et al., 1995). The KAx3 cells moved with an average instantaneous velocity of 10.4 ± 3.1 μm/min (n = 21), comparable to previously reported rates of translocation (Wessels et al., 1991). The *myoA*$^-$/*B*$^-$ and *myoB*$^-$/*C*$^-$ cells moved at 6.0 ± 3.6 (n = 16) μm/min and 6.1 ± 1.6 μm/min, respectively. These values are not significantly different from those reported for the *myoA*$^-$ and *myoB*$^-$ single mutants (Wessels et al., 1991; Titus et al., 1993).

Defects in development have been previously observed in strains that are impaired in pinocytic activity (O'Halloran and Anderson, 1992; Bacon et al., 1994). The ability of the mutant strains to complete development was evaluated by plating cells on nonnutrient agar plates at high density. The suspension-grown KAx3 strain formed normal mounds at 12 h (Fig. 11 *A*), whereas both of the suspension-grown myosin I double mutants formed abnormally shaped mounds (Fig. 11, *B–C*). These appeared to be less compact and smaller in the *myoA*$^-$/*B*$^-$ strain (Fig. 11 *B*), and irregularly shaped in the *myoB*$^-$/*C*$^-$ strain (Fig. 11 *C*). Both of the mutant strains formed fruiting bodies within 24–30 h after the onset of starvation, although these were substantially smaller than those formed by the KAx3 strain (Fig. 11, *D–F*). The developmental defect is also conditional. Cells grown on substrate closely resemble wild-type and single mutant cells throughout the developmental time course, producing fruiting bodies that closely resemble those of KAx3 cells (data not shown; Jung and Hammer, 1990; Peterson et al., 1995).

Discussion

The phenotypes of the *Dictyostelium myoA*$^-$/*B*$^-$ and *myoB*$^-$/*C*$^-$ myosin I double mutants—conditional defects in pinocytosis, membrane internalization, and growth, as well as a defect in manipulation of the actin cytoskeleton, are consistent with an impairment of plasma membrane/cytoskeleton function. Observation of FITC-dextran internalization by the double mutant cells has shown that these cells contain fewer fluid-filled vesicles per cell (Fig. 4). Consistent with these findings, ultrastructural analysis of myosin I double mutants taken directly from suspension indicates that the double mutants contain fewer large endocytic vesicles than wild-type cells (Fig. 5). Finally, the amount of membrane internalized by the double mutants is greatly reduced (Fig. 8). This defect probably results in reduced uptake of required nutrients, resulting in slower growth rates (Table I). The induction of the pinocytosis phenotype occurs immediately upon placing the double

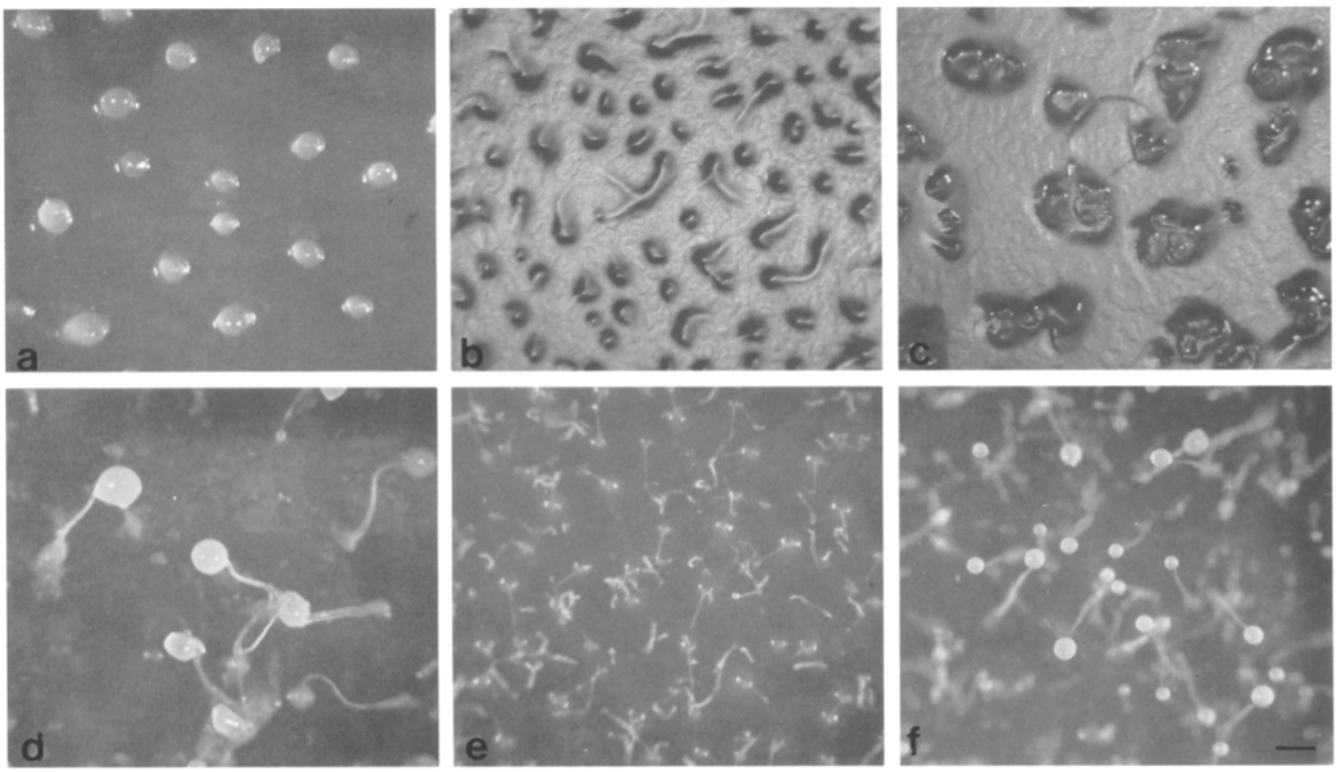

Figure 11. Suspension-grown myosin I double mutants appear altered during development. The KAx3 (*A* and *D*), *myoA*$^-$/*B*$^-$ (*B* and *E*) and *myoB*$^-$/*C*$^-$ (*C* and *F*) strains were taken from suspension, washed into nonnutrient medium and then plated on nonnutrient agar plates at 2.5 × 10^7 cells/ml. Pictures were taken at the mound stage (12 h, *A–C*) and at the end of development (24 h, *D–F*). Bar, 500 μm.

mutants in suspension. However, the mutants are capable of undergoing other actin-based cell processes such as phagocytosis in suspension and cell growth on a substrate. These observations suggest that the phenotypes observed in the double mutants are not simply a result of a general cytoskeletal disruption, but that myosin Is are required for a specific actin-based process carried out by cells in suspension to internalize fluid and membrane.

The double mutant phenotype does not result from a simple additive effect of single mutant phenotypes. The *myoA*$^-$, *myoB*$^-$, *myoC*$^-$ single mutants are not defective in fluid or membrane uptake. The *myoA*$^-$ and *myoB*$^-$ single mutants do, however, have similar defects in pseudopod formation, producing two times more pseudopodia than their wild-type counterparts, and moving with decreased instantaneous velocities (Wessels et al., 1991; Titus et al., 1993). Surprisingly, the *myoA*$^-$/*B*$^-$ mutant does not exhibit a reduction in instantaneous velocity beyond that of either single mutant, as might be expected if the combined mutations had an additive effect. Because the *myoC*$^-$ single mutant is indistinguishable from wild-type in all assays employed, we predicted the phenotype of the *myoB*$^-$/*C*$^-$ mutant to be identical to that of the *myoB*$^-$ single mutant. More surprisingly, removal of these two myosin Is from the cell resulted in a mutant phenotype identical to the *myoA*$^-$/*B*$^-$ double mutant. These observations suggest that these three myosin Is play roles, only some of which are overlapping, in several different membrane-cytoskeleton functions.

The Aberrations Observed in the Myosin I Double Mutants Are Conditional

The myosin I double mutants grown on a substrate do not exhibit the endocytic defects observed when they are grown in suspension (Fig. 2). Other *Dictyostelium* mutant strains also exhibit conditional defects when transferred from a surface to suspension culture. One is the dysphagia mutant that can phagocytose bacteria on filters but not in suspension culture (Cohen et al., 1994). Another is the *Dictyostelium* conventional myosin mutant that is defective in cytokinesis in suspension but undergoes cell division on a substrate (De Lozanne and Spudich, 1987). Growth in suspension appears to make demands on the cytoskeleton that exaggerate defects in basic actin-based cell movements such as pinocytosis, phagocytosis, and cytokinesis.

Substrate attachment may stimulate a different mechanism of pinocytosis which does not require myosin Is. Ruffling and the number of F-actin filled projections decrease with time of attachment (Peterson et al., 1994). The reduction in number of ruffles, which may be important for pinocytosis in suspension, could be related to induction of a new form of pinocytosis. A separate means of pinocytosis, such as trapping and internalizing fluid beneath the cell, may be induced when *Dictyostelium* cells attach to a surface.

The Role of Myosin I in Endocytosis

The endocytic defects observed in the myosin I double mutants are only somewhat different from those of the clathrin heavy chain null cells (CHC$^-$) (O'Halloran and Anderson, 1992). The CHC$^-$ show a 75% reduction in the rate of fluid-phase pinocytosis (O'Halloran and Anderson, 1992), as opposed to a 60% reduction for the double mutants. The CHC$^-$ strain, however, lacks any clear vesicles and is devoid of contractile vacuoles (O'Halloran and Anderson, 1992).

The double mutant endocytosis defect may lie in the clathrin-mediated pathway in that control of cytoskeletal rearrangements by myosin I could affect the ability of a clathrin-coated vesicle to become internalized by the cell. There is morphological evidence for the association of actin filaments with coated pits (Salisbury et al., 1980), and biochemical evidence that actin-binding proteins may mediate the association of clathrin-coated vesicles with actin filaments (Kohtz et al., 1990). Myosin Is may link the membrane of the newly formed coated vesicle to actin cables, serving to pull the vesicle into the cell. Myosin Is may also control the tension of the F-actin cytoskeleton, affecting the ability of the clathrin-coated vesicle to pass through the meshwork beneath the plasma membrane. If myoA, B, and C do participate in clathrin-mediated endocytosis, their removal does not completely shut down this process as fluid-uptake is only reduced by 60% in the double mutants.

Myosin Is may also participate in clathrin-independent pinocytosis, which has been proposed to account for the remaining 25% of fluid internalized by CHC null cells (Ruscetti et al., 1994). However, because of the many additional defects in the CHC null cells, including the inability to osmoregulate and undergo normal secretion (Ruscetti et al., 1994), it is difficult to use these cells to determine exactly what percent of fluid uptake actually takes place via clathrin-coated vesicles. Some of the reduction in fluid endocytosis may be a secondary effect of problems in osmoregulation and secretion. Therefore, non–clathrin-based endocytosis may account for a larger proportion of fluid uptake in *Dictyostelium.* Several methods exist in mammalian cells to distinguish between the two different types of endocytosis, including K^+ depletion (Cupers et al., 1994), cytosol acidification (Sandvig et al., 1987), and cytochalasin treatment (Sandvig and van Deurs, 1990). The K^+ depletion and cytosol acidification methods are not available for *Dictyostelium* and will need to be developed. Furthermore, the *Dictyostelium* plasma membrane is impermeable to cytochalasins (McRobbie and Newell, 1985), so other methods to test the effect of general cytoskeletal disruption on pinocytosis will also have to be carefully tested.

One form of non–clathrin-mediated pinocytosis that myosin Is may participate in is macropinocytosis, a process where endocytic vesicles are derived from areas of the plasma membrane exhibiting extensive membrane ruffling (Racoosin and Swanson, 1992). Because such membrane extensions are known to be filled with F-actin, it is easy to picture the types of roles myosin Is could play in such a process. We have shown that removal of two myosin Is from cells results in defective cytoskeletal rearrangements and extensions of membrane as cells attach to a substrate (Figs. 8 and 9). The inability to control membrane extensions during attachment may reflect a defect in controlling the extension and retraction of membrane necessary for efficient macropinocytosis in suspension. For example, the production of a greater number of membranous extensions in suspension by the double mutants could result in

decreased fluid-phase pinocytosis by causing delays in the ability of the cell to efficiently internalize all of them. The apparent localization of a myosin I with these structures (Fig. 10) is consistent with the idea that myoB, and possibly other myosin Is, functions in formation or retraction of these processes.

The extension of too many membrane processes has been shown to affect other cell processes in *Dictyostelium*. The *myoA*$^-$ and *myoB*$^-$ single mutants, which produce twice as many pseudopodia as wild-type cells, exhibit a 50% decrease in instantaneous velocity and an increase in the number of turns executed by the cells (Wessels et al., 1991; Titus et al., 1993). The increased number of crowns produced by the double mutants (Table II; Fig. 9) correlates with a delayed reorganization of the actin cytoskeleton upon attachment to a substrate; the larger amount of actin sequestered in the crown structures must be retrieved and recruited to form the basal ring of actin that is observed in the wild-type cells. These defects may be a reflection of the types of disturbances in actin function that occur in cells undergoing pinocytosis in suspension.

What Do These Myosin Is Do?

There are at least two different roles that the myoA, B, and C motors could play in a model of pinocytosis in which actin filled projections extend, close over to enclose fluid, retract back into the cell, and traffic the fluid-filled vesicle into the cytoplasm. The first step in pinocytosis is the formation of an actin-rich membrane extension. This process is likely to be random and ongoing, possibly occurring by thermal motion of the plasma membrane coupled to actin polymerization and local osmotic swelling (Condeelis, 1993). The actin-rich membrane projection, therefore, is assumed to extend by release of stored G-actin monomers followed by polymerization at the plasma membrane and subsequent cross-linking of the actin filaments by actin binding proteins (Condeelis, 1993). The finding that *Dictyostelium* myosin I single and double mutants are capable of making actin-rich extensions such as pseudopodia and crowns (Wessels et al., 1991; Titus et al., 1993; this paper) strongly suggests that these motors do not provide the protrusive forces required for making these structures, in spite of the reported localization of myoB and myoC to the actin-rich leading edge of lamellipodia in chemotacting cells (Fukui et al., 1989; Jung and Hammer, 1994).

The myosin Is, anchored either on the plasma membrane or in the underlying actin cortex, may then serve to retract the actin-rich projections that have folded over to encapsulate fluid (Fig. 12 *A*). They could perform this function by generating sliding of the membrane or actin relative to membrane-attached actin filaments. Myosin Is associated with the membrane of the newly formed vesicle could then be used to initially propel the fluid-filled vesicle through the actin cortex and into the endocytic pathway (Fig. 12 *B*). After the vesicle transits the actin-rich cortex, the myosin Is could be released from the membrane and recycled back to the plasma membrane.

Alternatively, the myosin Is may provide a contractile force at the membrane/cortex boundary that would inhibit the extension of too many processes by providing sufficient contractile force to prevent outward deformation of the membrane (even if monomers were added to the barbed end of an actin filament, the filament would be pulled into the cortex). Release of the inhibitory contractile force provided by the myosin I would occur in a localized fashion, possibly by dephosphorylation of active myosin I heads (Fig. 12 *C*). The finding that the myosin I single mutants make an increased number of pseudopodia dur-

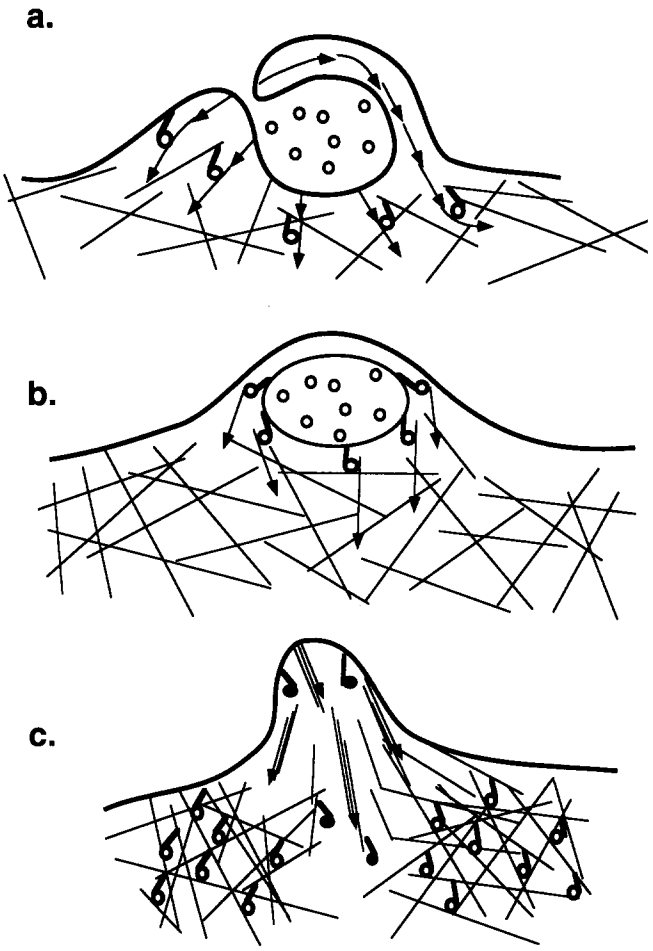

Figure 12. A schematic illustration of myosin I function in endocytosis and membrane extension. The top two panels illustrate an actin-filled membrane projection extending and closing over on itself, entrapping liquid, during pinocytosis. (*a*) The activated myosin Is (○‾) slide the extended membrane in the direction of the filament's pointed end (*arrowheads*) or pull membrane-attached actin filaments (*long arrows*, with the arrowhead indicating polarity of the filament) relative to each other to retract the fluid-filled projection. The straight lines represent the randomly oriented actin filaments present in the underlying cortex. (*b*) The activated myosin Is associated with the vesicle membrane propel the pinosome through the actin cortex toward and into the cytoplasm, where it subsequently enters the endocytic pathway. (*c*) An alternative model where active myosin Is (○‾) function to suppress formation of F-actin extensions by tightly cross-linking actin filaments in the cell cortex to prevent the outward projection of membrane. In areas where the myosin Is are inactive (●‾), the myosin Is are unable to provide a contractile force on the cortex, and the membrane is able to extend by the polymerization of actin filaments and subsequent bundling of the actin filaments by actin binding proteins.

ing translocation (Wessels et al., 1991; Titus et al., 1993) and that the double mutants make an increased number of crowns (Table II) provides support for a suppressing function for myosin Is. It is not possible to clearly rule out either a constraining or retracting role for myosin Is based on our current data, and neither of these possibilities are mutually exclusive. Myosin Is are likely to be involved in several different aspects of cytoskeletal rearrangements, and different isoforms may play dominant roles in any of these processes. It is apparent, however, that myoA, B, and C interact in a cooperative, nonredundant fashion to control events occurring at the membrane–cytoskeleton interface that are required for pinocytosis in suspension.

The authors especially wish to thank B. Luna for many stimulating discussions as well as for comments and insights that greatly improved the manuscript. Thanks also to Drs. D. Kiehart and B. Bacon for their helpful comments on the manuscript. We are grateful to M. Niswonger and T. O'Halloran for sharing the membrane internalization assay and for many discussions. Microscopic facilities were generously made available by Drs. D. Kiehart and M. Sheetz.

The initial portions of this work were supported by grants from the American Cancer Society (PF-3886 to M. D. Peterson; CB-90A and JFRA-378 to M. A. Titus) and the National Institutes of Health (AR14317-22 to M. K. Reedy). M. A. Titus is a member of the Duke Comprehensive Cancer Center.

Received for publication 24 May 1995 and in revised form 25 August 1995.

References

Adams, R. J., and T. D. Pollard. 1989. Binding of myosin I to membrane lipids. *Nature (Lond.).* 340:565–568.

Ausubel, F. M., R. Brent, R. E. Kingston, D. D. Moore, J. G. Siedman, J. A. Smith, and K. Struhl. 1993. *In* Current Protocols in Molecular Biology. New York, John Wiley and Sons.

Bacon, R. A., C. J. Cohen, D. A. Lewin, and I. Mellman. 1994. *Dictyostelium discoideum* mutants with temperature-sensitive defects in endocytosis. *J. Cell Biol.* 127:387–399.

Bähler, M., R. Kroschewski, H. E. Stöffler, and T. Behrmann. 1994. Rat myr4 defines a novel subclass of myosin I: identification, distribution, localization, and mapping of calmodulin-binding sites with differential calcium sensitivity. *J. Cell Biol.* 126:375–389.

Baines, I. C., and E. D. Korn. 1990. Localization of myosin IC and myosin II in *Acanthamoeba castellanii* by indirect immunofluorescence and immunogold electron microscopy. *J. Cell Biol.* 111:1895–1904.

Baines, I. C., H. Brzeska, and E. D. Korn. 1992. Differential localization of *Acanthamoeba* myosin I isoforms. *J. Cell Biol.* 119:1193–1203.

Bement, W. M., T. Hasson, J. A. Wirth, R. E. Cheney, and M. S. Mooseker. 1994*a*. Identification and overlapping expression of multiple unconventional myosin genes in vertebrate cell types. *Proc. Natl. Acad. Sci. USA.* 91:6549–6553.

Bement, W. M., J. A. Wirth, and M. S. Mooseker. 1994*b*. Cloning and mRNA expression of human conventional myosin-IC. A homologue of amoeboid myosin Is with a single IQ motif and SH# domain. *J. Mol. Biol.* 243:356–363.

Cohen, C. J., R. Bacon, M. Clarke, K. Joiner, and I. Mellman. 1994. *Dictyostelium discoideum* mutants with conditional defects in phagocytosis. *J. Cell Biol.* 126:955–966.

Condeelis, J. 1993. Life at the leading edge. *Annu. Rev. Cell Biol.* 9:411–444.

Cupers, P., A. Viethen, A. Kiss, P. Baudhuin, and P. J. Courtoy. 1994. Clathrin polymerization is not required for bulk-phase endocytosis in rat fetal fibroblasts. *J. Cell Biol.* 127:724–735.

de Hostos, E. L., B. Bradtke, F. Lottspeich, R. Guggenheim, and G. Gerisch. 1991. Coronin, an actin binding protein of *Dictyostelium discoideum* localized to cell surface projections, has sequence similarities to G protein β subunits. *EMBO (Eur. Mol. Biol. Organ.) J.* 10:4097–4104.

De Lozanne, A., and J. A. Spudich. 1987. Disruption of the *Dictyostelium* myosin heavy chain gene by homologous recombination. *Science (Wash. DC).* 236:1086–1091.

Demerec, M., E. Adelberg, A. Clark, and P. Hartman. 1966. A proposal for a uniform nomenclature in bacterial genetics. *Genetics.* 54:61–67.

Doberstein, S. K., and T. D. Pollard. 1992. Localization and specificity of the phospholipid and actin binding sites on the tail of *Acanthamoeba* myosin IC. *J. Cell Biol.* 117:1241–1249.

Dowrick, P., P. Kenworthy, B. McCann, and R. Warn. 1993. Circular ruffle formation and closure lead to macropinocytosis in hepatocyte growth factor/scatter factor-treated cells. *Eur. J. Cell Biol.* 61:44–53.

Drenckhahn, D., and R. Dermietzel. 1988. Organization of the actin filament cytoskeleton in the intestinal brush border:a quantitative and qualitative immunoelectron microscope study. *J. Cell Biol.* 107:1037–1048.

Fath, K., and D. R. Burgess. 1993. Golgi-derived vesicles from developing epithelial cells bind actin filaments and possess myosin-I as a cytoplasmically-oriented peripheral membrane protein. *J. Cell Biol.* 120:117–127.

Fukui, Y., S. Yumura, and T. K. Yumura. 1987. Agar-overlay immunofluorescence: high-resolution studies of cytoskeletal components and their changes during chemotaxis. *Methods Cell Biol.* 28:347–356.

Fukui, Y., T. J. Lynch, H. Brzeska, and E. D. Korn. 1989. Myosin I is located at the leading edge of locomoting *Dictyostelium* amoebae. *Nature (Lond.).* 341: 328–331.

Fukui, Y., J. Murray, K. S. Riddelle, and D. R. Soll. 1991. Cell behavior and actomyosin organization in *Dictyostelium* during substrate exploration. *Cell Struct. Func.* 16:289–301.

Goodloe-Holland, C. M., and E. J. Luna. 1987. Purification and characterization of *Dictyostelium discoideum* plasma membranes. *Methods Cell Biol.* 28:103–128.

Goodson, H. V., and J. A. Spudich. 1995. Identification and molecular characterization of a yeast myosin I. *Cell Motil. & Cytoskeleton.* 30:73–84.

Hadwiger, J. A., and R. A. Firtel. 1992. Analysis of $G_\alpha 4$, a G-protein subunit required for multicellular development in *Dictyostelium. Genes & Dev.* 6:38–49.

Howard, P. K., K. G. Ahern, and R. A. Firtel. 1988. Establishment of a transient expression system for *Dictyostelium discoideum. Nucleic Acids Res.* 16: 2613–2623.

Hulen, D., A. Baron, J. Salisbury, and M. Clarke. 1991. Production and specificity of monoclonal antibodies against calmodulin from *Dictyostelium discoideum. Cell Motil. and Cytoskeleton.* 18:113–122.

Ingalls, H. M., C. M. Goodloe–Holland, and E. J. Luna. 1986. Junctional plasma membrane domains isolated from aggregating *Dictyostelium discoideum* amebae. *Proc. Natl. Acad. Sci. USA.* 83:4779–4783.

Jung, G., and J. A. Hammer, III. 1990. Generation and characterization of *Dictyostelium* cells deficient in a myosin I heavy chain isoform. *J. Cell Biol.* 110: 1955–1964.

Jung, G., and J. A. Hammer, III. 1994. The actin binding site in the tail domain of *Dictyostelium* myosin IC (myoC) resides within the glycine- and proline-rich sequence (tail homology 2). *FEBS (Fed. Eur. Biochem. Soc.) Lett.* 342: 197–202.

Jung, G., C. L. Saxe, III, A. R. Kimmel, and J. A. Hammer, III. 1989. *Dictyostelium discoideum* contains a gene encoding a myosin I heavy chain isoform. *Proc. Natl. Acad. Sci. USA.* 86:6186–6190.

Jung, G., Y. Fukui, B. Martin, and J. A. Hammer, III. 1993. Sequence, expression pattern, intracellular localization and targeted disruption of the *Dictyostelium* myosin ID heavy chain isoform. *J. Biol. Chem.* 268:14981–14990.

Klein, G., and M. Satre. 1986. Kinetics of fluid-phase pinocytosis in *Dictyostelium discoideum* amoebae. *Biochem. Biophys. Res. Commun.* 138:1146–1152.

Kohtz, D. Z., V. Hanson, and S. Puszkin. 1990. Novel proteins mediate an interaction between clathrin-coated vesicles and polymerizing actin filaments. *Eur. J. Biochem.* 192:291–298.

Kuspa, A., and W. F. Loomis. 1992. Tagging developmental genes in *Dictyostelium* by restriction enzyme-mediated integration of plasmid DNA. *Proc. Natl. Acad. Sci. USA.* 89:8803–8807.

Lynch, T. J., J. P. Albanes, E. D. Korn, E. A. Robinson, B. A. Bowers, and H. Fujisaki. 1986. ATPase activities and actin binding properties of subfragments of *Acanthamoeba* myosin IA. *J. Biol. Chem.* 261:17156–17262.

Maeda, Y., and T. Kawamoto. 1986. Pinocytosis in *Dictyostelium discoideum* cells. *Exp. Cell Res.* 164:516–526.

Manstein, D. J., M. A. Titus, A. DeLozanne, and J. A. Spudich. 1989. Gene replacement in *Dictyostelium*: generation of myosin null mutants. *EMBO (Eur. Mol. Biol. Organ.) J.* 8:923–932.

McRobbie, S. J., and P. C. Newell. 1985. Effects of cytochalasin B on cell movements and chemoattractant-elicited actin changes of *Dictyostelium. Exp. Cell Res.* 160:275–286.

Miyata, H., B. Bowers, and E. D. Korn. 1989. Plasma membrane association of *Acanthamoeba* myosin I. *J. Cell Biol.* 109:1519–1528.

Mooseker, M. S., J. S. Wolenski, T. R. Coleman, S. M. Hayden, R. E. Cheney, E. Espreatico, M. B. Heintzelman, and M. D. Peterson. 1991. Structural and functional dissection of a membrane-bound mechanoenzyme: brush border myosin I. *Curr. Top. Membr.* 38:31–55.

Morgan, N. S., D. M. Skovronsky, S. Artavanis-Tsakonas, and M. S. Mooseker. 1994. The molecular cloning and characterization of *Drosophila melanogaster* myosin-IA and myosin-IB. *J. Mol. Biol.* 239:347–356.

O'Halloran, T. J., and R. G. W. Anderson. 1992. Clathrin heavy chain is required for pinocytosis, the presence of large vacuoles, and development in *Dictyostelium. J. Cell Biol.* 118:1371–1377.

Pawson, T., and G. Gish. 1992. SH2 and SH3 domains: from structure to function. *Cell.* 71:359–362.

Peterson, M. D., and M. A. Titus. 1994. F-actin distribution of *Dictyostelium* myosin I double mutants. *J. Euk. Microbiol.* 41:652–657.

Peterson, M. D., K. D. Novak, M. C. Reedy, J. I. Ruman, and M. A. Titus. 1995. Molecular genetic analysis of myoC, a *Dictyostelium* myosin I. *J. Cell Sci.* 108:1093–1103.

Pollard, T. D., and E. D. Korn. 1973. *Acanthamoeba* myosin. I. Isolation from

Acanthamoeba castellanii of an enzyme similar to muscle myosin. *J. Biol. Chem.* 248:4682–4690.

Racoosin, E. L., and J. A. Swanson. 1992. M-CSF-induced macropinocytosis increases solute endocytosis but not receptor-mediated endocytosis in mouse macrophages. *J. Cell Sci.* 102:867–880.

Rosenfeld, S. S., and B. Rener. 1994. The GPQ-rich segment of *Dictyostelium* myosin IB contains an actin binding site. *Biochemistry.* 33:2322–2328.

Ruscetti, T., J. A. Cardelli, M. L. Niswonger, and T. J. O'Halloran. 1994. Clathrin heavy chain functions in sorting and secretion of lysosomal enzymes in *Dictyostelium discoideum. J. Cell Biol.* 126:343–352.

Ryter, A., and C. deChastellier. 1977. Morphometric and cytochemical studies of *Dictyostelium discoideum* in vegetative phase. Digestive system and membrane turnover. *J. Cell Biol.* 75:200–217.

Sandvig, K., and B. van Deurs. 1990. Selective modulation of the endocytic uptake of ricin and fluid phase markers without alteration in transferrin endocytosis. *J. Biol. Chem.* 265:6382–6388.

Sandvig, K., S. Olsnes, O. Petersen, and B. van Deurs. 1987. Acidification of the cytosol inhibits endocytosis from coated pits. *J. Cell Biol.* 105:679–689.

Salisbury, J. L., J. S. Condeelis, and P. Satir. 1980. Role of coated vesicles, microfilaments, and calmodulin in receptor-mediated endocytosis by cultured B lymphoblastoid cells. *J. Cell Biol.* 87:132–141.

Sussman, M. 1987. Cultivation and synchronous morphogenesis of *Dictyostelium* under controlled experimental conditions. *Methods Cell Biol.* 28:9–29.

Temesvari, L., J. Bush, M. Peterson, K. Novak, M. Titus, and J. Cardelli. 1996. Examination of endosomal and lysosomal pathways in *Dictyostelium discoideum* myosin I mutants. *J. Cell Sci.* In press.

Titus, M. A., H. M. Warrick, and J. A. Spudich. 1989. Multiple actin-based motor genes in *Dictyostelium.Cell Regul.* 1:55–63.

Titus, M. A., K. D. Novak, G. P. Hanes, and A. S. Urioste. 1995. Molecular genetic analysis of *myoF*, a new *Dictyostelium* myosin I gene. *Biophys. J.* 68: 152s–157s.

Titus, M. A., D. Wessels, J. A. Spudich, and D. Soll. 1993. The unconventional myosin encoded by the *myo*A gene plays a role in *Dictyostelium* motility. *Mol. Biol. Cell.* 4:233–246.

Urrutia, R. A., G. Jung, and J. A. Hammer. 1993. The *Dictyostelium* myosin-IE heavy chain gene encodes a truncated isoform that lacks sequences corresponding to the actin binding site in the tail. *Biochem. Biophys. Acta.* 1173: 225–229.

Wagner, M. C., B. Barylko, and J. P. Albanesi. 1992. Tissue distribution and subcellular localization of mammalian myosin I. *J. Cell Biol.* 119:163–170.

Wessels, D., J. Murray, G. Jung, J. A. Hammer, III, and D. R. Soll. 1991. Myosin IB null mutants of *Dictyostelium* exhibit abnormalities in motility. *Cell Motil. & Cytoskel.* 20:301–315.

Witke, W., M. Schleicher, and A. A. Noegel. 1992. Redundancy in the microfilament system: abnormal development of *Dictyostelium* cells lacking two F-actin cross-linking proteins. *Cell.* 68:53–62.

Yonemura, S., and T. D. Pollard. 1992. The localization of myosin I and myosin II in *Acanthamoeba* by fluorescence microscopy. *J. Cell Sci.* 102:629–642.

Zhu, Q., and M. Clarke. 1992. Association of calmodulin and an unconventional myosin with the contractile vacuole complex of *Dictyostelium discoideum. J. Cell Biol.* 118:347–358.